Spacelike distance from discrete causal order

Spacelike distance from discrete causal order

David Rideout
Perimeter Institute for Theoretical Physics
31 Caroline Street North, Waterloo,
Ontario N2L 2Y5, Canada

Petros Wallden
Raman Research Institute
Sadashivanagar, Bangalore - 560 080, India
(Dated: June 13, 2013)

Any discrete approach to quantum gravity must provide some prescription as to how to deduce continuum properties from the discrete substructure. In the causal set approach it is straightforward to deduce timelike distances, but surprisingly difficult to extract spacelike distances, because of the unique combination of discreteness with local Lorentz invariance in that approach. We propose a number of methods to overcome this difficulty, one of which reproduces the spatial distance between two points in a finite region of Minkowski space. We provide numerical evidence that this definition can be used to define a 'spatial nearest neighbor' relation on a causal set, and conjecture that this can be exploited to define the length of 'continuous curves' in causal sets which are approximated by curved spacetime. This provides some evidence in support of the "Hauptvermutung" of causal sets.

Contents

I. INTRODUCTION

One of the central problems which confronts every discrete/combinatorial approach to quantum gravity (see for example [1, 2, 3, 4, 5, 6, 7, 8]) is that of the so-called 'inverse problem' [9], which may be decomposed into two aspects. One regards the question as to how smooth continuum-like structures emerge from the underlying discrete dynamics. Implicit in this is a second, that of how to recognize that we have something which is smooth and continuum-like, if we did? The paper addresses this second question, by proposing a means to extract spatial distances and other geometric information from a causal set. Along with earlier prescriptions for measuring timelike distances from a discrete causal order [1, 10][1], these results give promise to specifying the full spacetime geometry (aka metric) from a causal set. This contributes towards the 'Hauptvermutung' (central conjecture) of causal set theory, which claims that two distinct, non-isometric spacetimes cannot arise from a single causal set.

A. Causal Sets

Causal Sets is one of the major approaches to constructing a theory of quantum gravity, and is perhaps the most minimalist in its starting point. The causal set hypothesis asserts that a discrete set of 'atoms of spacetime', endowed with merely a partial order relation, underlies the continuum, and provides the basis for a consistent quantum description of spacetime. The basic assumptions are that spacetime is *fundamentally discrete*, and that to this one need add only causal ordering of the elements to recover the full spacetime structure, including dimension, topology, differential structure, and metric, at macroscopic scales.

Several of the recent developments that have occurred in this approach at the kinematical level are [12, 13, 14, 15], at dynamical level [16, 17], and at the phenomenological level [18, 19]. For reviews see *e.g.* [20, 21, 22, 23]. Perhaps the greatest piece of evidence in support of the hypotheses underlying the causal set program to date is the successful prediction of the order of magnitude of the cosmological constant. In 1990 Rafael Sorkin argued that, from very general principles of spacetime discreteness, and the complementarity of spacetime volume and a cosmological constant in the gravitational action, one should expect a non-zero, fluctuating cosmological constant, whose magnitude was at the time just beyond the bounds of experimental observation [20, 24] (and believed to be vanishing by much of the scientific community). Note that this implied that an exactly vanishing cosmological constant was highly unlikely (if not ruled out) by causal sets.

Mathematically a causal set (or causet) is a set C endowed with a partial order relation $\prec$ which is irreflexive ($x \not\prec x$), transitive ($x \prec y \prec z \implies x \prec z$), and locally finite $[x, z] \equiv (|\{y|x \prec y \prec z\}| < \infty \; \forall \quad x, z \in C)$ (where $|A|$ indicates cardinality of the set A). The local finiteness condition imposes the requirement of discreteness, because it requires that there is only a finite number of elements between every pair in the causet. The quantity $[x, y]$ used to define local finiteness, which is the collection of elements following x but preceeding y in the partial order, is called a *causal interval* or simply *interval*, and plays an important role in the following. It is also sometimes called an Alexandrov neighborhood or Alexandrov set. A *link* is a relation between two elements which is not implied by transitivity, an 'irreducible relation'. A *chain* is a sub-causal set for which every pair of elements is related. An *antichain* is a subcauset which contains no relations. The term *n-antichain* is shorthand for an antichain containing n elements. The past of an element x past(x) is the set of elements $y \in C$ such that $y \prec x$. Similarly the future of an element x fut(x) is the set of elements $y \in C$ such that $x \prec y$. An element is called *minimal* if its past is empty. An element is called *maximal* if its future is empty.

Causal sets are fundamentally discrete, which means that one does not expect the spacetime continuum to arise as a continuum limit of the theory. What we should be seeking is a continuum *approximation*, which is some continuum spacetime that approximates the underlying fundamental discrete structure. To this end, we say that a particular spacetime approximates a causal set via the definition of a *faithful embedding*. A faithful embedding is a map ϕ from a

[1] This list of references is by no means complete. Timelike distance in a causal set has been studied from wide variety of perspectives, including the study of random permutations, the mathematics of random order structures, the optimization of algoirthms for accessing data off hard drives, and efficiency of airplane boarding strategies. For a more complete survey of the vast literature on this subject, see [11] and the references therein.

causal set C to a spacetime M that *(a)* preserves the causal relation (*i.e.* $x \prec y \iff \phi(x) \prec \phi(y)$) and *(b)* is 'volume preserving', meaning that the number of elements mapped to every spacetime region is Poisson distributed, with mean the volume of the spacetime region in fundamental units, and *(c)* M does not possess curvature at scales smaller than that defined by the 'intermolecular spacing' of the embedding. As mentioned above, the central conjecture of causal set theory is that a causal set cannot be *faithfully* embedded into two distinct, non-isometric spacetimes. However, the recovery of the corresponding metric and of some analogue of the differential structure from the causal set is still an open problem.

Throughout the paper we will need to refer to elements both of the embedding manifold and of the embedded causal set. To help clarify the discussion, we will reserve the term 'points' for the events of spacetime, and use 'element' to refer to the elements of the causal set.

The results presented here are purely kinematical in nature, that is they make no reference to any particular scheme for formulating a quantum dynamics for causal sets. Thus we expect them to be useful regardless of one's attitude toward 'quantization'. The notion of a faithful embedding provides a relatively concrete prescription with which to associate a continuum spacetime with a causal set, at the kinematical level. This concreteness is useful in allowing one to address kinematical questions, such as recovery of spatial distance from a causal set, independently of one's approach toward formulating quantum dynamics. In particular, since local Lorentz invariance already holds at the microscopic level, there is no need to recover it dynamically via some 'quantum superposition'. In fact it has been argued that *any* fundamentally discrete approach to quantum gravity must in some way contain a combinatorial structure which closely resembles a causal set, if that theory hopes to describe a continuum which posseses the macroscopic symmetries of Minkowski space [25].

Most of the results described in this paper are for causal sets which are well approximated by Minkowski spacetime. We point out that Minkowski spacetime is very important on its own right, for a variety of reasons:

- Curved spacetime is locally flat. Therefore the results obtained are important for understanding the small scales of causal sets that are approximated by a curved spacetime.[2]
- Most of particle physics is done for quantum matter in flat spacetime. Thus our first attempts at defining quantum field theory on a causal set background will be on causal sets which faithfully embed into Minkowski space. A definition of spatial distance on a causal set can be useful in formulating the dynamics, *e.g.* in writing down an action for fields on a causet background [26]. An alternative approach is to write down an action based upon non-local but causal differential operators defined on the causal set, as described in [19, 23]. Additionally, recent progress has been made in formulating the causal propagator for massive particles propagating on a causal set [17]. Perhaps a better understanding of spatial distance can be of use in formulating the Feynmann propagator.
- For the universe in which we live, spacetime is almost flat at the largest scales.
- In a model of full 2-d quantum gravity of causal sets [16], the main contribution from the sum over histories comes from causets which correspond to an interval in $\mathbb{M}^2$. While this is a toy model, it provides another reason to be interested in causal sets which are approximated by Minkowski spacetime.

B. Outline of this paper

In section II we review the well understood notion of timelike distance on a causal set, a first attempt at defining spatial distance, and the reason for the latter's failure. In section III we explore numerically the aforementioned timelike and spacelike distance measures. In section IV we proceed by considering some spatial geometrical information that we *can* recover from a causal set. We define n-links and discuss the dimension and 'manifoldness' information they may contain. We define 'generalized spatial distance', which is the radius of the minimum bounding sphere of d points in d-dimensions. Using a definition of 'equidistant elements', we recover the 'sphere distance', which is the diameter of a sphere circumscribed by d points in d-spacetime dimensions. All these definitions are tested numerically. Then in section V we suggest a new proposal for spatial distance, which does not suffer from the problems of previous suggestions. This is the main result of the paper. In section VI we show how we can compute closest neighbors from this distance. From this definition we may be able to define the length of continuous (timelike or spacelike) curves on a causal set, which generalizes to curved spacetime. We summarize and conclude in section VII.

---

[2] Note that this 'small scale' may be after some coarse graining of the causal set, to get to the macroscopic, continuum-like scales. It is of course quite open what the smallest scales of the causal set will look like.

II. ELABORATIONS ON EARLIER IDEAS

Given a spacetime manifold, it is easy to generate a causal set which will faithfully embed into it. One simply 'sprinkles' elements uniformly (with respect to the volume measure) at random, and then deduces the relations among the elements from the causal structure of the spacetime. Going the other way is much more difficult. One of the major tasks of causal set kinematics is to learn to deduce properties of the approximating continuum merely from the order relation.

The recovery of the spacetime manifold that approximates the causal set, using only the partial ordering of the elements, has not been fully achieved. Much is understood about how to compute the dimension [22, 27], and more recently the spatial topology [13]. In the following, we will review some early works on the timelike distance (proper time) [1, 2, 10] and spatial distance, since this is what we will be dealing with in the rest of the paper.

A. Timelike distance

Following [10], we define proper time $d(x, y)$, between two related elements $x \prec y$, to be the number of links L in the *longest* chain between (and including) x and y[3].

$$d(x, y) := L$$

Thus to compute this, one considers all chains starting from x and ending at y, and counts the number of links in (one of[4]) the largest one(s). This definition is intrinsic to the causal set, and does not depend on whether it can be faithfully embedded into a manifold, nor on the expected dimension of such a manifold. In [10] (and references therein) it is shown that, in the case of a casual set C which arises by a sprinkling of density ρ into d-dimensional Minkowski space[5] (so one gets a faithful embedding $\phi : C \to M$), the distance $d(x, y)$ is proportional to the proper time between the endpoints $\phi(x)$ and $\phi(y)$. In particular the authors state that

$$L(\rho V)^{-1/d} \to m_d \quad \text{as} \quad \rho V \to \infty \,, \tag{2.1}$$

for some constant m_d which depends upon the dimension. Here V is the spacetime volume of the causal interval $J^+(x) \cap J^-(y)$ ($J^{\pm}(x)$ represents the causal future/past of x respectively). The exact value of m_2 is known to be 2, while for other dimensions some bounds exist: $1.77 \leq m_d \leq 2.62$.

It is known that in two dimensions the variance in L grows as $N^{1/3}$ (slower than the naive $L \sim N^{1/2}$ that one might expect) [28]. Furthermore, the next-to-leading order term in the asymptotic behavior (2.1) is also known. It turns out that the expected value $\langle L \rangle$ underestimates the limit (2.1) by a term proportional to $N^{-1/3}$ [28]. We make use of this fact in fitting our numerical results of section III A.

Given a causet that is faithfully embedded in d-dimensional Minkowski spacetime, one can easily extract timelike distance in another manner, taking direct advantage of the number-volume correspondence of the causal set [2]. Consider again a timelike separated pair of causet elements $x \prec y$. Associated with this pair is an Alexandrov interval in $\mathbb{M}^d$, $J^+(\phi(x)) \cap J^-(\phi(y))$, whose volume V_{xy} is simply

$$V_{xy} := \int_{J^+(x)\cap J^-(y)} d^d z = \eta(d) \times l_{xy}^d \tag{2.2}$$

where l_{xy} indicates the 'spacetime interval', *i.e.* the proper time separation between x and y. The coefficient is given by

$$\eta(d) = \frac{2V_{d-1}^s}{2^d d} \,,$$

---

[3] Note that the Lorentzian character of the partial order is manifested in this definition. Graphs (of 'finite valence'), on the other hand, naturally embed into Euclidean spaces, and hence one generally defines distance in terms of *shortest* paths on a graph.

[4] For a sprinkling into Minkowski space, the number of longest chains will generally be very large, in fact it grows exponentially with the length of the chain.

[5] Note that we are abusing notation here, by using the same symbol d for the dimension of Minkowski space and distance. We expect that the meaning will be clear from context.

where V_n^s is the volume of a unit n-ball. We can use this simple fact to compute the proper time between causal set elements x, y, by counting the number of elements in the causal interval $[x, y]$, and inverting (2.2). We will call this distance *volume distance*.

Volume distance has a number of advantages over counting the length of the longest chain, in that it is exact for finite regions, and, since it effectively integrates over a large region of the causet, has considerably smaller fluctuations. Some disadvantages are that it is more explicitly dependent upon dimension, and it is not clear how to make use of such a definition in the context of an inhomogeneous spacetime. We will at times take advantage of volume distance in the sequel, for convenience, though for the most part we stick with the arguably more fundamental method of counting chains to measure timelike distance in the causal set. In principle either definition of timelike distance can be used in the constructions described herein. Note that volume distance is used in the construction of ref. [14], which seeks to recover the faithful embedding in $\mathbb{M}^d$ from the causal set, since there the accuracy for finite regions is quite important.

B. Spacelike distance

The situation is quite different for spacelike distance. Previously (*e.g.* [2, 10]) a suggestion for what might be spacelike distance was brought forward. Along with this suggestion came the reason why in general this would fail for a causal set. We will thus use the term *naive spatial distance* for this proposal, since the authors of [10] themselves rejected it. An important note is that we restrict our attention here to Minkowski spacetime. In section VI we will mention possible generalizations to curved spacetime.[6]

Given two unrelated elements x, y one defines the naive spatial distance $d_{ns}(x, y)$ to be given by the minimum timelike distance between an element w in their common past and another z in their common future. Thus $w \prec (x, y) \prec z$, and

$$d_{ns}(x, y) := \min_{w,z} d(w, z) \ .$$

The timelike distance can be calculated using either the length of the longest chain or volume distance. The motivation for this definition comes from the fact that in Minkowski spacetime, the minimum timelike distance from the common past to the common future of two spacelike points x, y, is indeed their spacelike distance. This proposal works for a causal set that is approximated by 2-d Minkowski spacetime. However, it fails in higher dimensions.

In 1+1 dimensions, for a given pair of points x, y, there is a unique pair of points $w \prec x, y$ and $z \succ x, y$ (in the continuum) which are separated by the minimum proper time. We therefore expect to find $O(1)$ pairs of elements w, z (in the causal set) which have a minimum timelike separation, and the smallest of these should be a good estimate for the spatial separation between $\phi(x)$ and $\phi(y)$, for a faithful embedding $\phi : C \to \mathbb{M}^2$. However, in higher dimension, there will be an infinite number of such pairs of points w, z, each separated by the same minimum proper time. It is this infinity of pairs which causes difficulty in a discrete setting.

To see in detail why naive spatial distance fails to recover spacelike distance for causal sets which faithfully embed into $\mathbb{M}^d$ for $d > 2$, let us first consider the situation in the continuum. We have a pair of spacelike points x, y, and seek pairs of elements w in their common past and z in their common future, for which the timelike distance along the geodesic connecting w and z is shortest. Such a point w will necessarily lie on the intersection of x and y's past light cones, and z on the intersection of their future light cones. For any such point w, there will be a unique z which minimizes the timelike distance. We call such a pair of points a *continuum minimizing pair*. As mentioned above, in 1+1 dimensions there is a unique such pair w, z, while in higher dimension the intersections of the light cones will form a surface of co-dimension 2, and since for each of these points in the past there exists a corresponding one in the future which forms a continuum minimizing pair, we find an infinite number of such pairs.

For a causal set which is faithfully embedded into $\mathbb{M}^d$, it is clear that there will be in general pairs of causal set elements 'close'[7] to each continuum minimizing pair. In section V we will properly define a discrete analogue of a minimizing pair in a causal set. For the moment we will rely on the above intuitive description of 'discrete minimizing pairs', as elements $w \in \text{past}(x) \cap \text{past}(y)$ and $z \in \text{fut}(x) \cap \text{fut}(y)$ which are close to some continuum minimizing pair.

An important point is that proper time for each minimizing pair w, z (measured in whichever way) depends upon the contents of the causal interval $[w, z]$. Since every such interval must necessarily contain the elements x and y,

---

[6] It should be highlighted here that even the concept of spacelike distance itself is not unambiguously defined for curved spacetime. However, the length of a spacelike curve *is* well defined.

[7] The precise definition of 'close' is not important at this stage. We can use a Euclidean metric on the embedding space, for example.

they all overlap. However, the extent of overlap (as measured by cardinality, or spacetime volume in the faithful embedding) can be made arbitrarily small by considering causal intervals which are related by a sufficiently large boost. We call such minimizing pairs *independent minimizing pairs*. (See figure 1 for an illustration.) Since this is

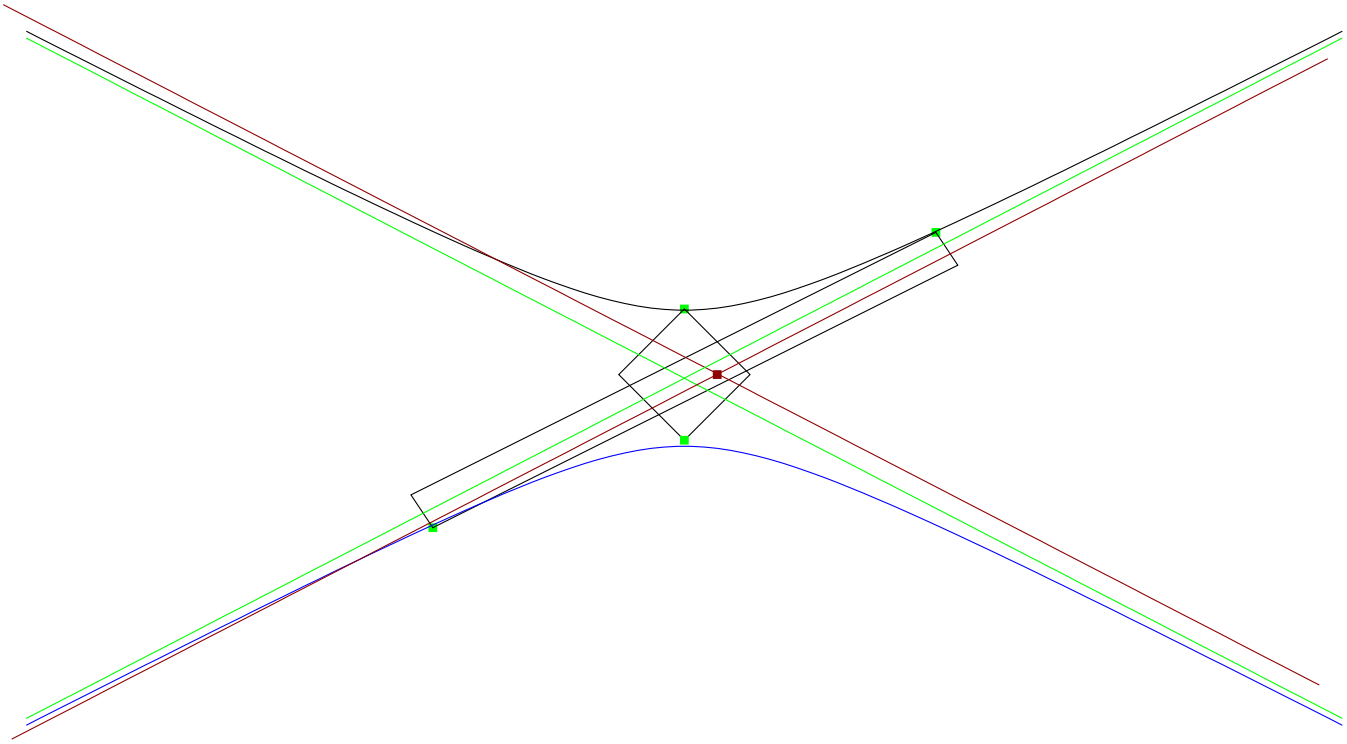

FIG. 1: Illustration of two intervals associated with two minimizing pairs in a sprinkling into $\mathbb{M}^3$. The elements x and y lie at the center of the figure, but displaced out of and into the page by some finite equal amount. The hyperbolae indicate the intersection of the past and future light cones of x and y. The long straight green lines are the asymptotes of the hyperbolae. The green dots with black intervals indicate the projection of two causal intervals for minimizing pairs onto the plane of the page. Please ignore the red dot in the center of both intervals, along with the pair of red lines which pass through this dot. These will be used in section IV B.

true of any pair of such intervals $[w_1, z_1]$ and $[w_2, z_2]$, it is clear that the infinite collection of intervals $[w_i, z_i]$ sample an infinite volume of Minkowski space[8]. Thus, because the probability of a sprinkling exactly two elements into an interval of any size is non-zero, with probability 1 we will find some intervals (in fact an infinite number) which contain only the elements x, y, and thus when minimizing over all pairs we will get a trivial distance of 2 (for either method of computing timelike distance) for *any* unrelated pair x, y.

Many similar proposals have been considered for spacelike distance, but all suffer a similar fate. Spatial distance in a discrete, Lorentz invariant context has unfamiliar subtle difficulties. One can make progress by breaking the Lorentz invariance, as we consider in section IV. In section V, we replace the minimum above with an average over suitably selected minimizing pairs, and present numerical evidence that this is sufficient to overcome the difficulties described above.

---

[8] In case the reader is still not convinced, let us be more explicit as follows: Consider one continuum minizing pair w_i, z_i (a pair of points $w_i \in J^-(x) \cap J^-(y)$ and $z_i \in J^+(x) \cap J_+(y)$ whose (timelike) geodesic distance is minimum), with its corresponding interval $[w_i, z_i] \equiv J^+(w_i) \cap J^-(z_i)$, and a second pair w_j, z_j with its interval $[w_j, z_j]$. These intervals will have a finite overlap $[w_i, z_i] \cap [w_j, z_j]$. Now select any finite overlap threshold T. There will exist an infinite number of pairs/intervals $[w_k, z_k]$ which have an overlap $\mathrm{Vol}([w_i, z_i] \cap [w_k, z_k]) \leq T$. Now select one of these $[w_k, z_k]$, and repeat the argument, to find another interval with arbitrarily small overlap with the first two. Repeating this argument an infinite number of times leads to an infinite number of intervals with arbitrarily small overlap among themselves. (Note that one has to be careful not to have repeats in the sequence of intervals which this algorithm yields. It is clear that this is possible, *e.g.* in $\mathbb{M}^3$ by 'always going in the same boost direction' to find new intervals. In higher dimension there will obviously be more 'arbitrarily independent intervals' than in $\mathbb{M}^3$.)

III. DETAILS OF SIMULATIONS

Here we present some simulations which show how the timelike and spacelike distance measures described in section II perform 'in practice'. These simulations were all performed using a CausalSets toolkit within the Cactus high performance computing framework [29]. The Monte Carlo simulations are facilitated by a MonteCarlo toolkit in Cactus, which provides a variety of methods for generating independent parallel random numbers within the Cactus framework. For the computations described in this work, the random numbers were generated via a multiple recursive linear congruential generator proposed by L'Ecuyer [30].[9]

In all our simulations we generate a causal set by sprinkling into some finite convex region of Minkowski space. Such a causal set obviously comes with a faithful embedding into that same region. We use this embedded causal set to test the various measures of timelike and spatial distances described in the paper.

In order to select elements of the causal set between which we seek to measure distances, we simply select a number of *target points* in $\mathbb{M}^d$, and choose the causal set elements which are nearest the target points, using a (flat) Euclidean metric.[10] We should stress that this procedure is of no fundamental importance, which is why we are justified in using a Euclidean metric, which is frame dependent, and also using the embedding in such an explicit way. It is simply a procedure for selecting, in a practical and easy manner, elements from the causal set on which we can employ our distance measures. As the sprinkling density goes to infinity, the continuum distance between a target point and the location to which the nearest element is mapped in the faithful embedding goes to zero.

For some of our simulations we do not use a proper Poisson sprinkling, in that we hold the total number of sprinkled elements N fixed. For large N this very closely approximates a true Poisson sprinkling. In fact, for all the values of N used in this paper, the results for a fixed N sprinkling are indistinguishable from those for a full Poisson sprinkling. (This is partially due to the fact that our fluctuations are greater for smaller causets, and these greater fluctuations overwhelm any effect due to fluctuations in the total causet size.) In other simulations we allow the total number of elements to vary with respect to a Poisson distribution, which is characterized by some mean value $\langle N \rangle$.

The results displayed in figures 2, 3, 6, 7, 10, and 12 all come from sprinklings with a fixed total number of elements. Those displayed in figures 5, 8, 13, 14, and 15 come from genuine Poisson sprinklings. In figure 4 we use a fixed N sprinkling for all but the largest three data points shown; for those three the indicated value of N represents the mean of the Poisson distribution. Our results are split in this way simply because we updated the 'sprinkling engine' of the CausalSets toolkit during the course of our simulations for this paper, primarily to check if it had any affect on our results. Where the size of the causal set has been randomized, it is to be understood throughout that N (and $N_\diamond$ etc.) stands for the mean of the appropriate Poisson distribution, rather than a value from one sampling of it.

Most all results we present are from a Monte Carlo simulation in which we generate causal sets 'one off', and compute the distance measures as described. In the case that the distance measure is undefined for the particular randomly generated causal set, we simply discard it from our statistics (though we still count it against the total number of causets to generate, so this occurrence will tend to lead to larger error bars). This can occur because the selected antichain does not have any elements it its common future or past, or does not possess any future 2-links (see below).

A. Timelike Distance

For starters we consider (finite density) sprinklings into an interval of $\mathbb{M}^2$. Note that almost surely elements of the causal set will not get mapped to the endpoints of the interval. We instead use the endpoints of the interval as target points, so we use the closest elements in the sprinkling to define an interval $[x, y]$ within the causal set. Here we could have taken a different approach, as in ref. [10], in which one conditions on there being causal set elements at the 'endcaps' of the interval. We prefer this approach because it more closely resembles the computations we do later for various measures of spatial distances, without imposing any condition on the embedding.

Here let us highlight why we should not use Lorentzian distance when finding the elements closest to the target points (end-points in this case). Imagine in 1+1-dimensions an interval, starting from $(t = -1, x = 0)$ (call it point A) and finishing at $(t = +1, x = 0)$ (point B). If we use Lorentzian distance to find the element closest to A, it may turn out to be an element close to $(0, -1)$, since this point is close to the lightcone of A. Similarly we may get for

[9] Note that there appears to be a sign error in L'Ecuyer's implementation of his algorithm. We use the parameters specified in the main text of the article, rather than those used in his implementation.

[10] The more typical procedure in this regard is to condition on the presence of causet elements at the target points (*e.g.* at the endpoints of a causal interval). We instead choose to sprinkle without such conditions.

point closest to B an element close to $(0,+1)$. However, these 'nearby' points not only do not give us a good idea of the longest chain in the interval between A and B, they are not even related in the first place! This is avoided by using the Euclidean metric.

In the following we use $N_\diamond$ to refer to the mean cardinality of $[x,y]$, and $V_\diamond$ to refer to the spacetime volume of the interval in the continuum $[\phi(x),\phi(y)]$. N and V correspond to the (mean) total number of elements in the interval we sprinkle, and the total spacetime volume into which we sprinkle, respectively. As $N\to\infty$ the ratio $\frac{V_\diamond}{V}=\frac{N_\diamond}{N}\to 1$.

We wish to use length (number of links) of the longest chain L between the elements x, y to estimate the timelike geodesic separation T_c between the corresponding points in the manifold $\phi(x),\phi(y)$. Using the theorem from reference [10]

$$\frac{L}{N_\diamond^{1/d}}\to m_d\ ,$$

in probability in the asymptotic limit $\rho\to\infty$, and the fact that the volume $V_\diamond$ of a spacetime interval in d dimensions is given by

$$V_\diamond = D_d T^d$$

(where D_d is an $O(1)$ constant factor, in particular for our purposes we will need $D_2=\frac{1}{2}$ and $D_3=\frac{\pi}{12}$), one can estimate the timelike separation in the manifold by

$$T=\frac{L}{m_d\rho^{1/d}D_d^{1/d}}\ . \tag{3.1}$$

This is of course valid only in the limit $\rho\to\infty$. For finite ρ, (3.1) consistently underestimates the continuum distance T_c. We refer to such underestimation as *timelike underestimation*. (In fact, to leading order, in 1+1 dimensions, this underestimation is known to fall off as one over the variance in L).

For the relatively miniscule sizes of causal sets which can be put on a computer (*e.g.* $N\ll 10^{64}$), the deviation for finite ρ is important. To account for this, we replace the ratio m_d by an 'effective ratio'

$$m_d^{\text{eff}}=\frac{L}{(\rho V_\diamond)^{1/d}}\ . \tag{3.2}$$

As we can easily see, in the limit $\rho\to\infty$, we have $m_d^{\text{eff}}\to m_d$. Ideally we would like a functional form of an effective m_d which would behave correctly at all scales. This has not been calculated analytically (though much is known for the 2-dimensional case). Here we compute L numerically and estimate the functional form of m_d^{eff} by curve fitting. In particular, for each sprinkled causal set, we compute the length of the longest chain between our 'nearest pair' x and y, and from that compute the quantity m_d^{eff} from (3.2).

In figure 2, we test how well the length of longest chain approximates the timelike distance, in $\mathbb{M}^2$, if we use the known asymptotic value of $m_2=2$. In particular, we perform a sequence of simulations, each of which sprinkles 900 causal sets into an interval of fixed height T_i, in fundamental units. For each value of T_i, we plot a mean deviation $\left\langle\frac{T-T_c}{T_c}\right\rangle$, where T is as given in (3.1), and T_c is the continuum distance $\sqrt{-(\phi_t(y)-\phi_t(x))^2+(\phi_x(y)-\phi_x(x))^2}$ (where the subscript t,x on $\phi()$ indicates the time or space coordinate respectively). In addition we include the error bar for each mean, which we estimate in the usual manner from the sampled data values. As one expects, the mean deviation goes to zero as $T\to\infty$. We also note that for small distances, we observe considerable underestimation (the phenomenon we call timelike underestimation). In fact, even for relatively 'large' distances that are easily representable on a typical workstation, we still get a mean deviation of about 1.8% from the continuum proper time.

In order to show that our distance measures overcome the difficulty presented in section II B (and to avoid the comparatively large computational effort of simulations in 3+1 dimensions), we will perform most of our simulations in 2+1 dimensions. Since analytic results on the value of m_3 are restricted to bounds, and there are no results on the functional form for m_3^{eff} [11], we will need to compute these quantities numerically. For 'practice', we do this as well in 1+1 dimensions, where we know both the exact value of m_2 and the asymptotic form of m_2^{eff}.

In Figure 3 we plot various values of $\left\langle m_d^{\text{eff}}\right\rangle$ for dimension $d=2$, for 400 runs of the same simulations as described above, along with their standard error bars. Here we use the total number of elements in the causal set $N=T_i^2/2$ for the horizontal axis labels. The asymptote is, as stated in ref. [10], equal to 2. We fit the data points for $N\geq 2^6$, to the function

$$f(N)=m_d+aN^{b/\ln 2}\ . \tag{3.3}$$

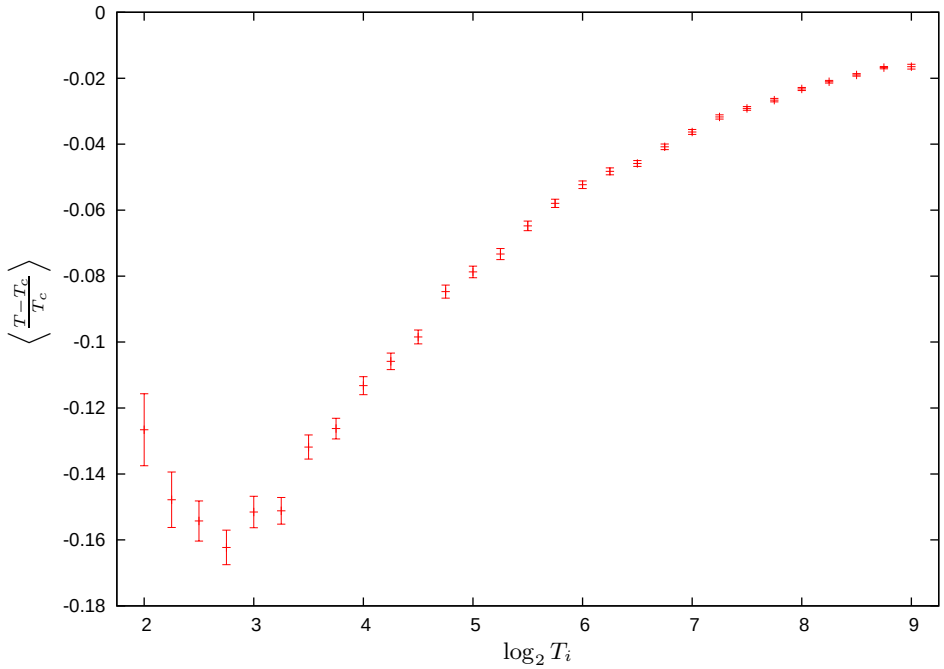

FIG. 2: Measurement of proper time between a pair of elements in a causal set sprinkled into variously sized intervals of $\mathbb{M}^2$, by counting the length of the longest chain. Each data point plotted indicates the mean deviation along with its standard error, for 900 runs.

The parameter values are $m_2 = 2.0102 \pm 0.0037$, $a = -0.791 \pm 0.041$, and $b = -0.1741 \pm 0.0077$. The errors are as output from gnuplot's fit command, which also gives $\chi^2 = 28.43$. Since it is not of central significance to the rest of the paper, we will not enter into the details of the curve fit, apart from getting a numerical estimate of the value of m_3. Here we see that we are able to reproduce the correct value of m_2 to within a half of a percent.

The functional form we guessed to fit our data (3.3) is exactly that of Odlyzko and Rains, as given in reference [28], with $a \approx -1.758$ and $b = -\frac{\ln 2}{3} \approx -.231049$ (and $m_2 = 2$). We include this function in figure 3, for reference. It appears that we are able to reach the asymptotic approximation, at the largest causal sets we have simulated. Note that any difference between our procedure and those of [10, 28] is washed out for the largest causets.

We are now in a position to repeat the analysis in 2+1 dimensions. In Figure 4 we again plot $\langle m_3^{\text{eff}} \rangle$ for sprinklings into an interval of $\mathbb{M}^3$. For the smaller simulations ($N < 2^{17}$), we generate 1600 causets for each value of N, while for the larger simulations we use fewer (400 at 2^{17} and $2^{17.5}$, 100 at 2^{18}). We again fit to the functional form (3.3), and find the parameter values $m_3 = 2.296 \pm 0.012$, $a = -1.087 \pm 0.014$, and $b = -0.1201 \pm 0.0053$. For almost all computations of a timelike distance using the length of the longest chain in this paper, we will use such a numerical approximation to m_3.[11] An exception is in demonstrating the failure of naive spatial distance in section III B 2, where we will need an acurate numerical measurement of timelike distance.

In figure 5 we test how measuring length of the longest chain differs from the continuum proper time in 2+1 dimensions, as we saw above in 1+1. In order to generate this plot we have used the asymptotic value of m_3^{eff}, *i.e.* $m_3 \approx 2.296$. Note that there is still a 6% deviation from the continuum distance, for the largest causets we simulate.

B. "Naive spatial distance" and its failure

In this section, we will examine the naive spatial distance, and demonstrate that the problem described in section II B is observable in computer generated causal sets. We recall that naive spatial distance was a successful distance

[11] In practice we will sometimes use a value we computed earlier, $m_3 \approx 2.278$, rather than the value above. Since the corresponding computations are only used to obtain qualitative results, the resulting 2% difference in timelike distances will have no affect on the conclusions of the paper.

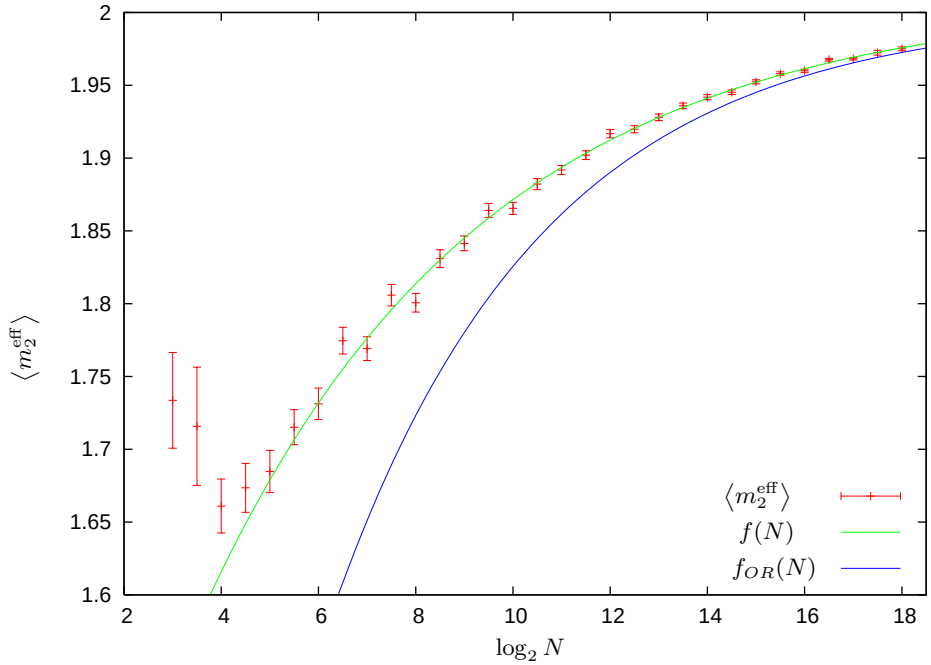

FIG. 3: Correction to (3.1) for finite causets. Here we measure m_2^{eff} by comparing with the known continuum timelike distance. $f_{OR}(N)$ is the leading order correction to the asymptotic value $m_2^{\text{eff}} = 2$ [28].

function for $\mathbb{M}^2$. However, in higher dimensions, it failed, due to the existence of an infinite number of independent minimizing pairs. In computer simulations, it is only possible to sprinkle into regions of finite volume, and therefore one can only consider causets which faithfully embed into a finite region of Minkowksi space. In a such finite region, there are only a finite number of minimizing pairs, and thus one cannot directly observe the failure of naive spatial distance (giving a trivial result). However, one *can* observe some underestimation of the distance. Here we demonstrate the latter, by considering a sequence of larger and larger subregions of $\mathbb{M}^3$, and observe the naive spatial distance decaying toward its trivial result.

In order to avoid confusion, we should stress here that we will have two different kind of plots. In section III B 1, we will consider how naive spatial distance is performing when we increase the density of sprinkling, while keeping the target points fixed. This means that the plots correspond to distances that vary in fundamental units (as in previous sections), and some effects will vanish in the limit of infinite distance in fundamental units. In section III B 2, however, we will keep the distance in fundamental units fixed, and only increase the size of the sprinkling region. This means that all the points of the plot in section III B 2 correspond to a single point in the other graphs, in particular to the point in which the distance between target points is 8 in fundamental units. This is why we should *not* expect to see the effect of timelike underestimation to vanish (and thus we need an accurate value for m_3^{eff}). Similarly, some other effects that vanish in the limit in which the distance goes to infinity in fundamental units must be taken into account in section III B 2.

1. *Numerical results for naive spatial distance*

We first consider how naive spatial distance performs in $\mathbb{M}^2$ and $\mathbb{M}^3$, for a fixed region in Minkowski spacetime, when sending the sprinkling density ρ to infinity.[12] Because the spacetime volume of the region is fixed, although the number of minimizing pairs will diverge with ρ, we expect the number of *independent* such pairs to remain roughly fixed. This is because, in order for two minimizing pairs to be independent, their corresponding intervals must have small overlap. Given that the spatial separation between the elements x and y are fixed, and the volume of the sprinkling region is fixed, there is only room for so many 'independent intervals', and thus the effective number of

[12] Equivalently we consider increasing distances in fundamental units.

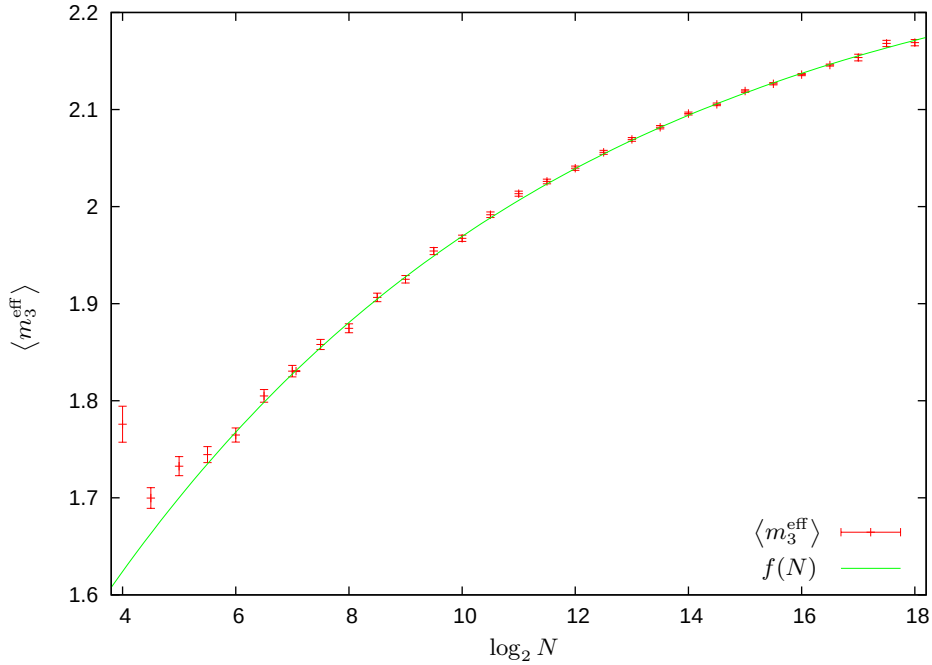

FIG. 4: Convergence of length of the longest chain to proper time, in an interval of $\mathbb{M}^3$. The fitting function shown is $f(N) = m_3 + a * e^{b \log_2 N}$.

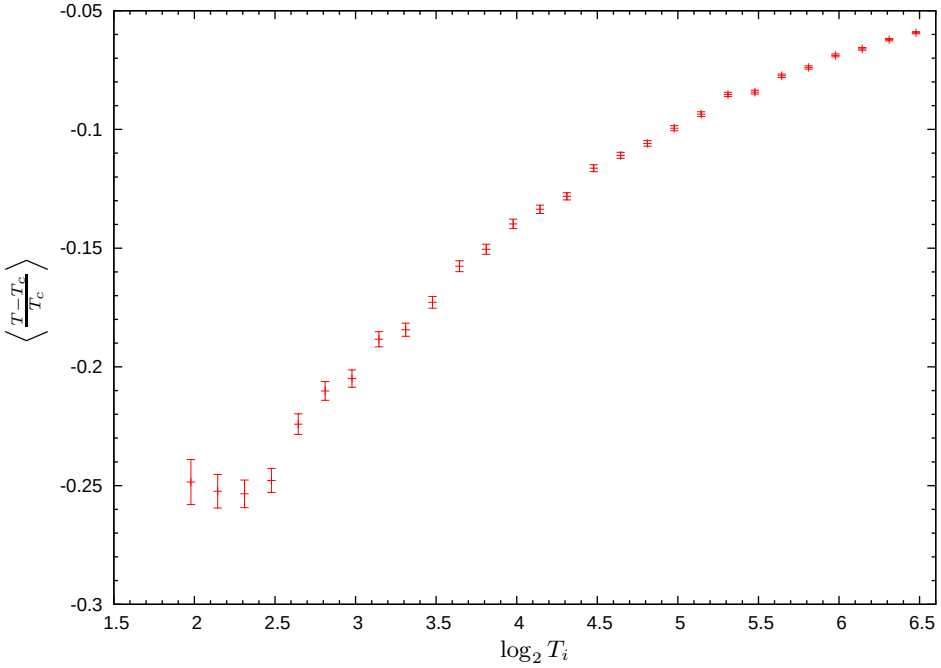

FIG. 5: Measurement of proper time of a sprinkled interval in $\mathbb{M}^3$, of various sizes.

minimizing pairs remains bounded. Thus we expect that naive spatial distance will perform reasonably well in this scenario of finite volume but diverging density.

In figure 6 we show the results of a sequence of simulations of 400 sprinklings into a fixed square of $\mathbb{M}^2$, at various densities. A point in the square takes coordinate values t and x in $(-1, 1)$. We choose target points at $(t = 0, x = \pm\frac{3}{10})$, and compare the spacelike distance X between the corresponding causet elements as described in section II B, with the continuum distance between their embedding locations X_c.

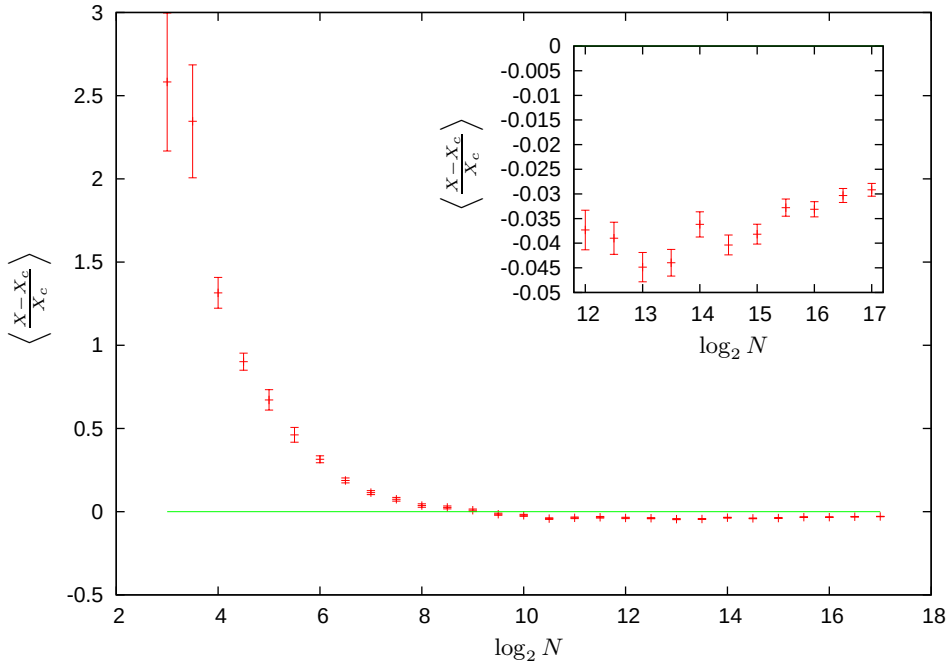

FIG. 6: Measurement of naive spatial distance in 1+1 dimensions. We sprinkle N elements into the Cartesian coordinate square $[-1,1]^2$. Target points are at $(t=0, x=\pm\frac{3}{10})$. The inset plot zooms in on the large N data, to show that the deviation is not constant, but behaves in a manner consistent with a drift toward zero.

The first thing to note is that for small N we encounter a significant overestimation, that quickly vanishes at larger N.[13] A possible reason for this is the fact that there will not exist causet elements exactly on the intersection of the relevant lightcones. The spacelike distance prescription selects minimizing pairs which are more distant than these lightcone intersections, thus leading to a larger estimate for spacelike distance. We will refer to this phenomenon as *spacelike overestimation*. Once we get to sufficiently large N that spacelike overestimation is negligible, then we observe (solely) the now familiar timelike underestimation. One may be concerned that it looks as if the deviation approaches a constant negative value. However, upon zooming into the large N data points, we see that the behaviour of the ratio is consistent with a drift toward zero, as one would expect. The slowness of the drift is due to the slow convergence of length of the longest chain to the timelike distance.

In figure 7 we show the analogous results for 400 sprinklings into a fixed cube of $\mathbb{M}^3$. The target points are $(t=0, x=\pm\frac{3}{10}, y=0)$. Here we use the (older) asymptotic value $m_3 \approx 2.278$. The plots show the same features as in 2 dimensions, namely the existence of spacelike overestimation, timelike underestimation, and also the fact that the deviations seem consistent with a slow drift toward zero in the asymptotic limit.

2. *Demonstration of failure of naive spatial distance*

Recall that naive spatial distance fails due to the existence of a large number of minimizing pairs, whose corresponding intervals have small mutual overlap (*i.e.* independent minimizing pairs). In order to be able to "detect" the failure of the naive spatial distance we need to perform simulations which consider an increasing number of independent minimizing pairs. To achieve this we will need to sprinkle into a very large region. Furthermore we have noticed that there exists some underestimation from counting the length of the longest chain for timelike distance, which we called timelike underestimation. This underestimation is corrected by using a measured value for m_3^{eff}, rather than the asymptotic value m_3. There is also some overestimation that we have called spacelike overestimation (the effects of which explains the high values of the first points of figures 6 and 7).

With these issues in mind, we choose to sprinkle 900 causal sets into a box shaped region of $\mathbb{M}^3$, with coordinate

[13] Small N means equivalently small distance in fundamental units.

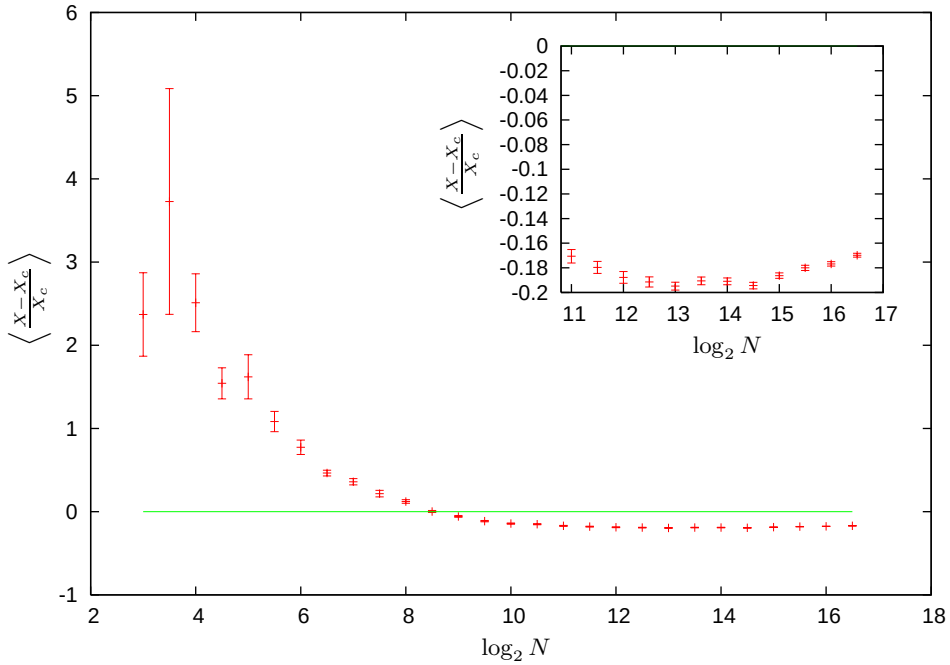

FIG. 7: Measurement of naive spatial distance in 2+1 dimensional Minkowski spacetime. We sprinkle into the Cartesian coordinate cube $[-1,1]^3$, at varying densities. Target points are at $(t=0, x=\pm\frac{3}{10}, y=0)$. The inset plot zooms in on the large N data, to show that the deviation is not constant, but is consistent with a slow drift toward zero.

values $t \in (-T,T)$, $x \in (-4,4)$, and $y \in (-T,T)$. The two target points are at $(t=0, x=\pm 4, y=0)$. We again measure the spatial separation X, and compare with the continuum value X_c. As T gets larger, we will capture increasingly longer portions of the intersection of the light cones, near which the minimizing pairs lie. Here we have chosen coordinates such that the sprinkling density ρ is fixed at 1. Thus the distance to be measured remains constant in fundamental units.

To overcome timelike underestimation, as mentioned above, we must carefully measure the relevant value of m_3^{eff}. Since the target points are separated by a distance of 8, we expect the resulting minimizing pairs to be separated by a distance of approximately 8. The corresponding interval then has a volume of $\frac{\pi}{12}8^3 \approx 134$. A careful (averaging over 250 000 causets) measurement of $m_3^{\text{eff}}(134)$ yields 1.83050 ± 0.00046.

Since it is a small distance (8 in fundamental units), and the timelike underestimation has been eliminated by using m_3^{eff}, we naively would expect to get a positive value for the deviation, due to spacelike overestimation. However, in figure 8, we see two things that stress the failure of the naive spatial distance. First, the value of the distance is *not* constant, but by merely considering successively larger regions of Minkowski space, we see its value reduce. The second is that, even though we have no reason to get a value below zero (*i.e.* an underestimation), we see that even within our computational powers, the value goes (systematically) negative. Therefore, taking into account more and more minimizing pairs not only balances the (relatively large for small distances) spacelike overestimation, but even produces some underestimation. In any event, this simulation confirms the well understood theoretical reason for the failure of the naive spatial distance.[14]

One potential loophole which may occur to the reader is that we may have used too small of a value of N (134), when computing the appropriate $m_3^{\text{eff}}(N)$, since the minimizing pairs will not fall exactly on the intersection of the light cones of x and y, but will be offset slightly from it (due to spacelike overestimation). Thus one may expect that we should use $m_3^{\text{eff}}(N)$) for some larger value than 134. A glance at figure 4 reveals that this would give a larger value for m_3^{eff}, and thus smaller values for X, which would have the affect of shifting the datapoints of figure 8 down by

[14] If we could send T to infinity, we would expect to see $L \to 2$, so $X = \frac{(\frac{12}{\pi})^{1/3} L}{m_3^{\text{eff}}} \to\sim 1.708$, and thus the deviation should converge to $(1.708-8)/8 \approx -.787$. To achieve the $L=2$ we would need a void in the sprinkling of volume $\sim 8^3$. The probability for this to occur for any given region of this volume is e^{-512}. Thus a rough estimate for the lower bound on the size of a sprinkling needed to reach $L=2$ is $N = 512\, e^{512}$, which is obviously far beyond our computational powers.

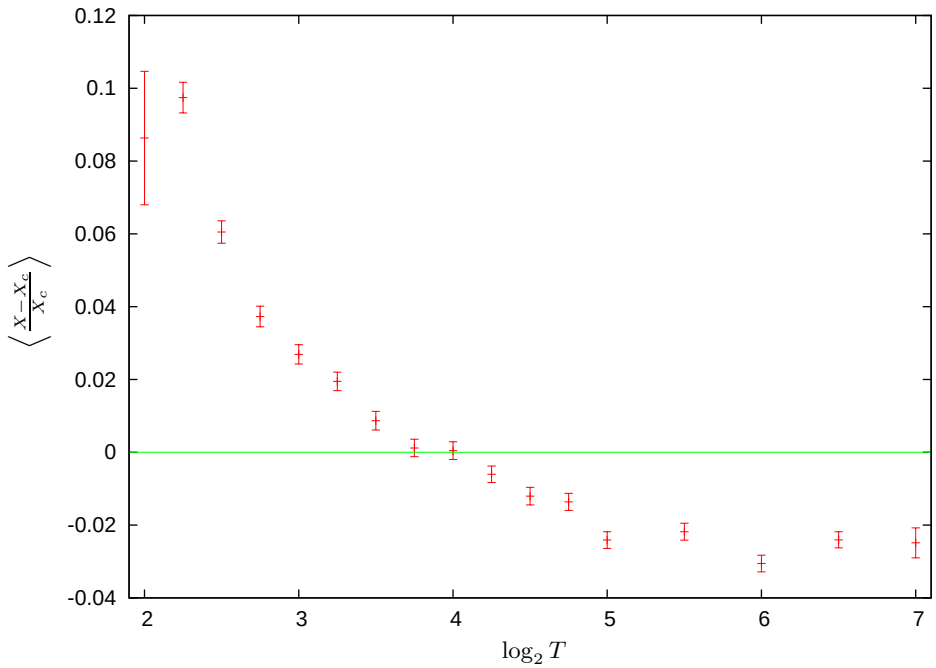

FIG. 8: Measurement of spatial distance for a pair of elements at fixed separation, while considering sucessively larger regions of $\mathbb{M}^3$. The sprinkling region has coordinates $t \in (-T, T), x \in (-4, 4), y \in (-T, T)$, with target points at $(t = 0, x = \pm 4, y = 0)$. The fact that the distance is not constant (decreases) and moreover crosses below zero shows that we are seeing the failure of the naive spatial distance, due to the existence of many minimizing pairs and the random fluctuations of the sprinkling generated causal set.

some amount. This merely strengthens the conclusion that we are seeing the failure of naive spatial distance in our simulations.[15]

IV. n-LINKS, SPHERE DISTANCE AND PROXIMITY

So far we have explored earlier attempts at defining a spatial distance measure on a causal set. In this section we proceed with some new considerations. Let us start with two definitions, the first in the continuum, and the second on a causal set.

Definition 1: The common future/past of a collection of n mutually spacelike separated points $\{x_i\}$ is

$$J_c^{\pm}(\{x_i\}) = \bigcap_{i=1}^{n} J^{\pm}(x_i) \tag{4.1}$$

Definition 2a: In a causal set, a *past n-link* of an n-element antichain $x_1, x_2, \cdots, x_n$ (n mutually unrelated elements) is an element y such that $y \prec x_m$ and $\nexists z$ such that $y \prec z \prec x_m$, for all $1 \leq m \leq n$.

Definition 2b: Similarly we define a *future n-link* of an n-element antichain $x_1, x_2, \cdots, x_n$ to be an element y such that $y \succ x_m$ and $\nexists z$ such that $y \succ z \succ x_m$ for all $1 \leq m \leq n$.

---

[15] One could also worry that, since the target points are at the edge of the sprinkling region, we will in fact see intervals with *smaller* N. We have checked for this explicitly by adding causet elements at the target points by hand, and found that this does not change the fact that we consistently see deviations less than zero, for large T.

A. n-links and the dimension

To gain an intuitive understanding of the meaning of these definitions, for causal sets which faithfully embed into $\mathbb{M}^d$, first consider the definition of a link in a causal set. A link is an 'irreducible connection' between a pair of (related) elements of a causet. By irreducible we simply mean that there are no intervening elements, and thus a link represents the shortest possible timelike distance between a pair of elements. Naturally this corresponds to the null relation in the continuum. Thus the collection of causet elements which are linked to a given element x will tend to lie very close to (while maintaining the causal relation) the past and future light cone of x.

Given this fact, one can intuitively understand the n-links as corresponding to sprinkled elements which are within, and close to, the light-cones of all n unrelated (*i.e.* spacelike) elements considered. Let us first explore the expected number of n-links of a given n-element antichain, in a causal set that has arisen as a sprinkling into $\mathbb{M}^d$. We will consider separately the cases where (a) $n > d$, (b) $n < d$, and finally (c) $n = d$. Note that we consider future n-links, but an identical analysis applies for past n-links.

The following equation yields the expected number of n-links in d dimensions.

$$\langle \#\ n-\text{links}\rangle = \rho \int_{J_c^+(\{x_i\})} dx^d \exp\{-\rho\, \mathrm{Vol}(J^-(x) \cap [\cup_{i=1}^n J^+(x_i)])\}\ ,$$

where $\mathrm{Vol}(R)$ indicates the spacetime volume of region R. The expression is simply a sum of independent random variables, each of which is the probability dx^d of finding a sprinkled element at x, times the probability that that element is linked to each of the x_i (so the region causally between x and the x_i must be empty of sprinkled elements). The region of integration is the common future $J_c^+(\{x_i\})$.

As an illustrative example, we will consider the expected number of future 2-links in 1+1 dimensions ($\mathbb{M}^2$). (Here and throughout the paper, when we speak of an expected number of n-links, it will always refer to the expected number of n-links of a given n-antichain.) Here we use fundamental units in which $\rho \equiv 1$. We choose our 2-antichain with $y_1 = (-r, -r)$ and $y_2 = (-r, r)$[16]. We get the integral

$$\langle \#\ 2-\text{links}\rangle = \int_0^\infty dt \int_{-t}^{t} dx \exp(-(t^2 + 4rt - x^2)/2)$$

since we subtract the overlap of the two regions $[y_1, x]_c$ and $[y_2, x]_c$.[17] By observing that, within the region of integration, $t^2 - x^2$ is positive and corresponds to the overlap of $[y_1, x]_c$ and $[y_2, x]_c$ we conclude that

$$\langle \#\ 2-\text{links}\rangle \leq \int_0^\infty dt \int_{-t}^{t} dx \exp(-2rt) = \frac{1}{2r^2}$$

This was possible since, in order to be a 2-link, the whole region $[y_1, x]_c \cup [y_2, x]_c$ had to be empty. If we require a subset of this region to be empty, we are guaranteed to get at least all the 2-links, along with some extra non-2-link elements. Therefore, this provides an upper bound on the number of 2-links. Note also that the above upper bound implies that the number of 2-links in $\mathbb{M}^2$, at most, falls off as $2/(2r)^2$, as the distance between the points $(2r)$ increases.

In $1+1$ dimensions we can easily see what happens to the expected number of 1-links (usually referred as links) and the 3-links. The former are infinite, as is well known. The expected number of 3-links will decrease as the distance between the points increases (as do the 2-links) but much more quickly. For example, choosing points $y_1 = (-r, -r)$, $y_2 = (-r, 0)$ and $y_3 = (-r, r)$, we get

$$\langle \#\ 3-\text{links}\rangle = \langle \#\ 2-\text{links}\rangle\ \exp\{-(r)^2/2\} \leq \frac{\exp\{-(r)^2/2\}}{(4r)^2}$$

which means that the expected number of 3-links drops exponentially faster than the 2-links, as the distance r between the points increases. By similar arguments for higher dimensions, we arrive at the following table, where the "$\to$", is understood as $r \to \infty$ (remember that r is in fundamental units).

---

[16] Admittedly we are conditioning on there being sprinkled elements at these points in spacetime, which is a zero probability event. However, we do not expect the results to change significantly if we instead use these points as target points, to select a pair of elements of the causet.

[17] We will refer to causal intervals in the continuum by $[y, x]_c$, and in these expressions x refers to a point in the domain of integration.

$\downarrow$n-link | dim $\rightarrow$	1+1	2+1	3+1
$\langle \#\ 1-\text{links}\rangle$	∞	∞	∞
$\langle \#\ 2-\text{links}\rangle$	$< 2/(2r)^2 \to 0$	∞	∞
$\langle \#\ 3-\text{links}\rangle$	$< \frac{\exp\{-(r)^2/2\}}{(4r)^2} \to 0$	$\to 0$	∞

These results generalize:

(a) $n > d$. In this case, typically we have no n-links. This means that for n unrelated elements, the probability of existence of an n-link is very small, and decreases rapidly for elements which are far from each other in the embedding. The n-link corresponds to an element that is just inside the lightcone of all n unrelated elements. If $n > d$, and none of the elements are very close to each other, there is no point (in the continuum) that can be only an ϵ distance from the light cones of all n elements. In the causal set, this is translated as a very small probability for existence of n-links.

(b) $n < d$. Here typically we will have infinite n-links (as for 1-links in 1+1, or 2-links in 2+1 dimensions). The reason is that in the continuum there exist a continuous infinity of points in the intersection of the lightcones, in particular a $(d-n)$-dimensional surface. Corresponding to each of these points there is a small but non-zero probability of a causal set element existing within a given, but arbitrarily small, distance. The infinity of such points in the continuum implies that there will be an infinite number of causal set elements close enough to give an n-link.

(c) $n = d$. In the continuum there exists a unique point that corresponds to the intersection of the n lightcones. In the faithfully embedded causal set, we expect there to be a non-zero but rather small probability (depending on the separation distance of the elements), as we have seen in the table, for a given d-antichain to possess a d-link.

Given these observations of the dependence of the behavior of n-links on dimension, it seems reasonable that counting of n-links could be used as a dimension estimator for causal sets. The idea would be roughly to select any n-antichain, for $n = 1$ (a single element), and count the number of links emanating from that element. Then increment n by one (select another unrelated element) and repeat. The first value of n for which one does not find a large number of n-links would be the dimension. In practice one may need to sample a number of antichains for each value of n in some manner.

In fact one can imagine that this itself may be a rather stringent necessary condition for a causal set to be 'manifoldlike', *i.e.* that it is likely to faithfully embed into some smooth spacetime manifold. If the numbers of n-links do not behave in the manner described above, then the causal set is not so likely to have the light cone structure that one expects from a continuum spacetime. Such a principle could be insightful in formulating a dynamics for causal sets, which yields faithfully embeddable causets, 'with high probability'.

B. Equidistant points, 'Sphere-distance' and l_g

As we have noticed earlier, the failure of the naive spatial distance was due to the existence of an infinite number of "minimizing pairs", in higher dimensions. Intuitively, this arises because in those higher dimensions, the locus of points (in the continuum) that lie exactly *on* both light-cones (of spacelike points $\{x_i\}$) is *not* a single point, but a full hyperboloid (a co-dimension 2 submanifold), and moreover one of infinite volume. The latter is important for the discrete case, since it would correspond to an infinite number of elements, while if the surface had finite volume in the continuum, it would correspond to only a finite number of elements of the causet.

Consider that this infinity of minimizing pairs arises because of Lorentz invariance. If we select two spacelike points of $\mathbb{M}^d$, then we have defined a system which remains invariant under a $d-2$ dimensional subgroup of the Lorentz group, namely those boosts which hold the pair of points fixed. In order to construct a non-trivial distance measure on a causal set, this suggests that we must select enough elements to eliminate this boost freedom of the system, *i.e.* we need a d-antichain. Note that the future (and also past) light cones of d spacelike points in $\mathbb{M}^d$ intersect at a single point[18], which suggests that the d-antichain may have a well defined distance measure associated with it. We consider two possibilities, which correspond to measuring the diameters of the bounding and circumscribing spheres defined by the d points.

[18] In the frame of simultaneity this reduces to finding the intersection of a collection of $d-2$-spheres of equal radius.

First we notice that the distance between the unique point on the d common future lightcones and the one on the past, corresponds to the diameter of the circumscribing[19] $d-2$ sphere. Unfortunately, we do not have an intrinsic way to find the element closest to the d common lightcones. (Here and throughout the paper, by the phrase "d common lightcones", or simply "common lightcones", we mean the intersection of the lightcones of the d spacelike points.) If past and future d-links existed, we could use those, but as we have seen in the previous section, in d-dimensions, in general, we find *no* d-links for an arbitrary selection of d unrelated elements.

An obvious choice is to use a procedure like the one in the naive spatial distance to locate this intersection point. We make the following definition.

Definition 3: Given d mutually unrelated elements x_i, we define the *generalized spatial distance* $l_g(x_1, \cdots, x_d)$ in d-dimensions, to be

$$l_g(x_1, \cdots, x_d) := \min_{w,z} d(w,z) \quad \text{where} \quad w \in J_c^-(\{x_i\}) \quad \text{and} \quad z \in J_c^+(\{x_i\})$$

However, minimizing over all the common future/past does not always 'select' the unique point of intersection of the light-cones. If it did, the distance recovered would be the diameter of the circumscribing $d-2$ sphere. Instead, the generalized spatial distance measures the diameter of the smallest $(d-2)$-sphere that *contains* (in the interior or on the boundary) the d spacelike elements (also known as "bounding sphere"). These two spheres coincide (in 2+1 dimensions) when the included angles at all the d elements (vertices) are acute, and in this case the minimizing pairs will tend to lie close to the intersection of the lightcones, so l_g should work well. In higher dimensions, an analogous statement will be true, with higher dimensional generalizations of the angles. In the case that the spheres disagree, however, a similar problem arises with the one in naive spatial distance, since we will find many, though not infinite, minimizing pairs. Since the minimizing pairs are many but not infinite, we expect some underestimation of the distance, though we should *not* get the trivial result of naive spatial distance.

To visualize the above, consider again figure 1, though this time there is a third element, at the red dot, which for convenience lies in the plane of the page. The projection of its lightcones with the page are drawn in red. For the computation of generalized spatial distance the minimizing pairs must also be related to this third element, so they are prevented from 'climbing' infinitely far up or down the left side of the hyperbolae. This makes the number of minimizing pairs finite. It also seems reasonable that, unless this third element lies extremely close to the line segment connecting the first two, the number of minimizing pairs will not even be large, so generalized spatial distance should still perform quite well.

To conclude, we can use the generalized spatial distance to accurately estimate the diameter of the bounding sphere, for unrelated elements that 'form acute angles'[20]. In other cases, we will get some underestimation, though we expect it to be extremely small in almost all circumstances. However, as of yet, we cannot know a priori whether the elements form obtuse or acute angles.

If one is more careful, it turns out to be possible to select a pair of elements which *will* yield the diameter of the circumscribing sphere. To describe the procedure, we first construct it in continuum Minkowski space.

We begin by defining our notation. Each point in Minkowski space is represented by a vector of its Cartesian coordinates

$$\mathbf{x}_i = (t^i, x_1^i, \cdots, x_{d-1}^i) \, .$$

The *spacetime distance* between any two points $\mathbf{x}_i, \mathbf{x}_j$ is defined to be

$$(\mathbf{x}_i\mathbf{x}_j)^2 = (t^i - t^j)^2 - (x_1^i - x_1^j)^2 - (x_2^i - x_2^j)^2 \cdots - (x_{d-1}^i - x_{d-1}^j)^2$$

If the distance is positive, the points are timelike separated, if negative they are spacelike, while if it is zero they are null.

Let us consider n spacelike separated points $\mathbf{x}_1, \mathbf{x}_2, \cdots, \mathbf{x}_n$.

Definition 4 : A point $\mathbf{w} \in J_c^{\pm}()$ is future / past n-equidistant with respect to the n spacelike points if

$$(\mathbf{w}\mathbf{x}_i)^2 = (\mathbf{w}\mathbf{x}_j)^2 \quad \forall \quad i,j = 1 \ldots n \, .$$

---

[19] The $d-2$ sphere that has all the d points on its boundary.

[20] From now on when we refer to 'acute angles' it is understood, in the case of higher dimensions, that the bounding sphere coincides with the circumscribing sphere.

We could have also define it alternatively (in fact equivalently in the continuum) by requiring that the corresponding volumes of the Alexandrov intervals match. The set of all such future / past n-equidistant points is labeled $\Theta_n^{\pm}$. Note that if $n > d$ we will typically find no n-equidistant points.

Definition 5 : We define the *n-equidistance* of a future / past n-equidistant point $\mathbf{y}$ with respect to n spacelike points $\mathbf{x}_1, \mathbf{x}_2, \cdots, \mathbf{x}_n$ to be the spacetime distance between the point $\mathbf{y}$ and any of the $\mathbf{x}_i$.

$$l_y^2 = (\mathbf{y}\mathbf{x}_i)^2 \ .$$

This of course is the same as the average over i of the spacetime distances $(\mathbf{y}\mathbf{x}_i)$.

Let us now derive an expression that relates past and future d-equidistances with the diameter, l_s, of the $(d-2)$-sphere which circumscribes d spacelike points.

Theorem: Given d spacelike points $\mathbf{x}_i$, in d-dimensional Minkowski spacetime, one past d-equidistant point $\mathbf{p}$ with equidistance l_p and one future d-equidistant point $\mathbf{f}$ with equidistance l_f, the spacetime distance $(\mathbf{pf})^2 := l_m^2$ goes as

$$l_m^2 = l_p^2 + l_f^2 + \frac{l_s^2}{2} + 2\sqrt{(l_p^2 + \frac{l_s^2}{4})}\sqrt{(l_f^2 + \frac{l_s^2}{4})} \ .$$

This equation can be solved for the diameter l_s

$$l_s = (l_m^4 + l_p^4 + l_f^4 - 2l_p^2 l_f^2 - 2l_m^2 l_p^2 - 2l_m^2 l_f^2)^{1/2}/l_m \ . \tag{4.2}$$

Proof. We first choose coordinates such that all the d spacelike points are in the $t = 0$ plane. Moreover we choose the origin $\mathbf{O}$ to be at equal spacelike distance from each of the d points, so that $\mathbf{x}_i = (0, x_1^i, \cdots, x_{d-1}^i)$, where $\sum_{n=1}^{d-1}(x_n^i)^2 = l_s^2/4$ for each of the $\mathbf{x}_i$. From the definition of equidistant point we have that the interval $(\mathbf{p}\mathbf{x}_i)^2$ goes as

$$(\mathbf{p}\mathbf{x}_i)^2 = (t^p)^2 - \sum_{n=1}^{d-1}(x_n^p - x_n^i)^2 = l_p^2$$

for all $i = 1 \ldots d-1$. From this we get that

$$\begin{aligned} \sum_{n=1}^{d-1} x_n^p(x_n^i - x_n^j) = 0 \qquad & \forall \quad i,j \in [1, d-1] \\ \mathbf{p}\cdot(\mathbf{x}_i - \mathbf{x}_j) = 0 \qquad & \forall \quad i,j \end{aligned}$$

using that $\sum_{n=1}^{d-1}(x_n^i)^2 = l_s^2/4$ for all $\mathbf{x}_i$'s. The dot in the above expression is the usual Minkowski inner product. Since the spatial components of the d spacelike points are arbitrary, almost certainly (*i.e.* with probability one) the $d-1$-surface at coordinate $t = 0$ is spanned by the $(d-1)(d-2)$ vectors of the form $\mathbf{x}_i - \mathbf{x}_j$. (For $d = 2$ we must replace the $(d-1)(d-2)$ vectors $(\mathbf{x}_i - \mathbf{x}_j)$ with the single vector $\mathbf{x}_1$.) From this, it follows that

$$x_n^p = 0 \quad \forall \quad n = 1, \ldots d-1 \ .$$

We now have that $\mathbf{p} = (t^p, 0, \cdots, 0)$, and by similar arguments $\mathbf{f} = (t^f, 0, \cdots, 0)$. We also have the equidistance to be

$$\begin{aligned} l_p^2 &= (t^p)^2 - l_s^2/4 \Rightarrow \\ t^p &= -\sqrt{l_p^2 + l_s^2/4} \end{aligned}$$

with the minus sign because it is *past* equidistant, and similarly for the future equidistant point (without the minus sign). We are now in a position to express the interval $(\mathbf{pf})^2 = l_m^2$ as a function of l_p, l_f and l_s.

$$\begin{aligned} l_m^2 &= (t^p - t^f)^2 \\ &= l_p^2 + l_f^2 + l_s^2/2 + 2\sqrt{l_p^2 + l_s^2/4}\sqrt{l_f^2 + l_s^2/4} \end{aligned}$$

Since this final expression is in term of only invariant quantities, it holds for all coordinates. □

It is now obvious that if we can define the above quantities for a causal set, we can use (4.2) to compute the radius of the $d-2$-dimensional circumscribing sphere of d unrelated elements.

Before defining (past/future) n-equidistant elements, and n-equidistance, for a causal set, let us note that n-links are essentially n-equidistant elements, with zero equidistance. They are by definition (when they exist) the closest equidistant elements.

Definition 6: Given n mutually unrelated elements of a causal set $x_1, \cdots, x_n$, we define future n-equidistant elements as the elements

$$w \in \bigcap_{i=1}^{n} \mathrm{fut}(x_i) \quad \text{such that} \quad |[x_i, w]| = |[x_j, w]| \quad \forall\, i, j = 1 \ldots n\ . \tag{4.3}$$

Past n-equidistant are defined equivalently, with $\mathrm{fut}(x_i)$ replaced by $\mathrm{past}(x_i)$. Note that here we have used volume distance, in place of the length of the longest chain, to locate equidistant elements. One can use the length of the longest chain as well, but it is much less efficient in locating the appropriate elements of the causal sets which give a good measurement of l_s.

Definition 7: We define the n-equidistance l_y^c of a (past/future) n-equidistant element w with respect to n unrelated elements $x_1, x_2, \cdots, x_n$ to be the volume distance between it and any of the x_i (all of which are equal, by definition 6).

$$(l_w^c) = |[x_i, w]|^{1/d}/D_d \tag{4.4}$$

The superscript 'c' will be dropped if there is no ambiguity.

One issue that is of concern is whether d-equidistant elements exist in causal sets which are faithfully embedable in $\mathbb{M}^d$, with respect to any d-antichain, and whether they are finite in number. It can be shown (see Appendix A) that in 1+1 dimensions there are an infinite number of equidistant elements. Based on this and on numerical simulations for higher dimensions, we conjecture that d-equidistant elements exist and are infinite in number, for any dimension.

Now we are now in a position to define the "sphere distance" associated with a $(d-2)$-sphere that is circumscribed by n spacelike elements. The quantity is defined intrinsically to the causal set, and has the property that there is no significant systematic over- or under-estimation at large distances.

Definition 8: Given d mutually unrelated elements $\mathbf{x}_i$ of a causal set, and any pair of their past $\mathbf{p}$ and future $\mathbf{f}$ d-equidistant elements, we define the *sphere-distance* $l_s(x_1, \cdots, x_d)$ to be given by (4.2) where the quantities l_m, l_p, l_f are computed using the volume distance of (2.2).

In numerical simulations we have used the past/future equidistant elements with smallest equidistance in order to compute l_s. However, in general one could use any pair of equidistant elements equally well. In our simulations the value obtained matched very closely with that deduced from the faithful embedding, *cf.* section IV C.

C. Numerical Results

In this section we test the "diameter measures" l_g and l_s on causal sets generated by sprinkling into an interval of $\mathbb{M}^3$. It is fairly straightforward to generalize the calculation to higher dimension, though the configurations considered would necessarily be more complicated, and we expect none of the results to change. In particular, we test l_g and l_s on two 'triangles' in $\mathbb{M}^3$, one obtuse (contains an included angle $> \frac{\pi}{2}$) and the other acute (all included angles $< \frac{\pi}{2}$). Here by a "triangle" we mean that we select three points in $\mathbb{M}^3$ as target points for sprinkled elements, which lie at the vertices of a triangle. Each of the triangles lie in the $t = 0$ plane.

Each simulation involves generating 100 causal sets, each with exactly the number of elements N as shown in figures 10 and 12. Since it is possible that, for any given causal set, one will not find both a past and future equidistant element, we introduce the notion of *equidistance quality*. The equidistance quality of a causet element w, with respect to a d-antichain $x_1, x_2, \ldots, x_d$, is given by

$$\sum_{x_i} \left(|[w, x_i]| - \langle |[w, x_i]| \rangle\right)^2\ , \tag{4.5}$$

where the sum indexes over the elements of the antichain x_i, and $\langle |[w, x_i]| \rangle$ is the mean of the quantities $|[w, x_i]|$. Note that for an ('exact') equidistant element w, this quantity will vanish. In our simulations we choose the closest[21]

[21] In practice we use the time coordinate of the embedding to decide which element is closest. Since, as stated earlier, it makes no difference which equidistant element one chooses, this should not affect our results. In any event we have never observed the collection of equidistant elements, as a sub-causal set, to form anything other than a chain. (Though we did not particularly look for this either.)

element for which the quantity (4.5) is as small as possible. Note that this extra definition is needed for purely practical reasons, given that we cannot sprinkle into the whole of Minkowski space. It seems clear that one will always be able to find elements of equidistance quality zero, *somewhere* in a sprinkling of the entirety of Minkowski space.

1. *Obtuse triangle*

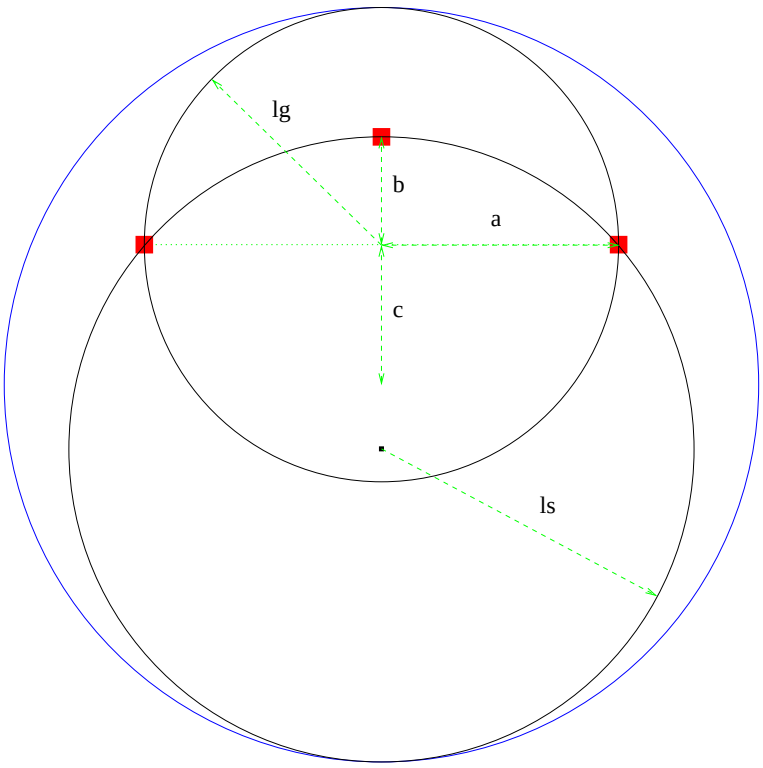

FIG. 9: Our obtuse triangle, in the $t = 0$ plane. In our coordinates $a = 2.2$, $b = 1$, $c = 1.42$. The causal set is sprinkled into the causal interval with endpoints $(t = \pm 6.5614, x = y = 0)$. The large blue circle is the intersection of the two lightcones which form the interval, and hence has radius 6.5614. (c is the distance between the center this largest bounding circle, and the center of circle which bounds the three target points.)

Figure 9 illustrates our obtuse triangle. For this configuration the continuum values of the diameter of the bounding and circumscribing spheres (circles in this case) are respectively $l_g = 4.4$ and $l_s = 5.84$. Note that these values are in arbitrary units, *not* in fundamental units. We consider successively larger sprinkling densities ρ, while holding the target points fixed. In figure 10 we demonstrate the following results: l_g converges (for large density ρ) to 4.4 as expected, while l_s converges to the value 5.84. The inset shows the asymptotic behavior in greater detail. For 'small triangles' / small ρ we observe the usual spacelike overestimation in l_g, and some small underestimation in l_s (for whatever reason).

2. *Acute triangle*

Figure 11 illustrates our acute triangle. For this configuration, the continuum values for the circumscribing and bounding sphere coincide at $l_g = l_s = 4.9193$. In figure 12 we demonstrate the following results: Both l_g and l_s converge to the continuum value 4.9193 (and therefore in the limit they coincide), but we can see from the inset that l_s converges more quickly than l_g.

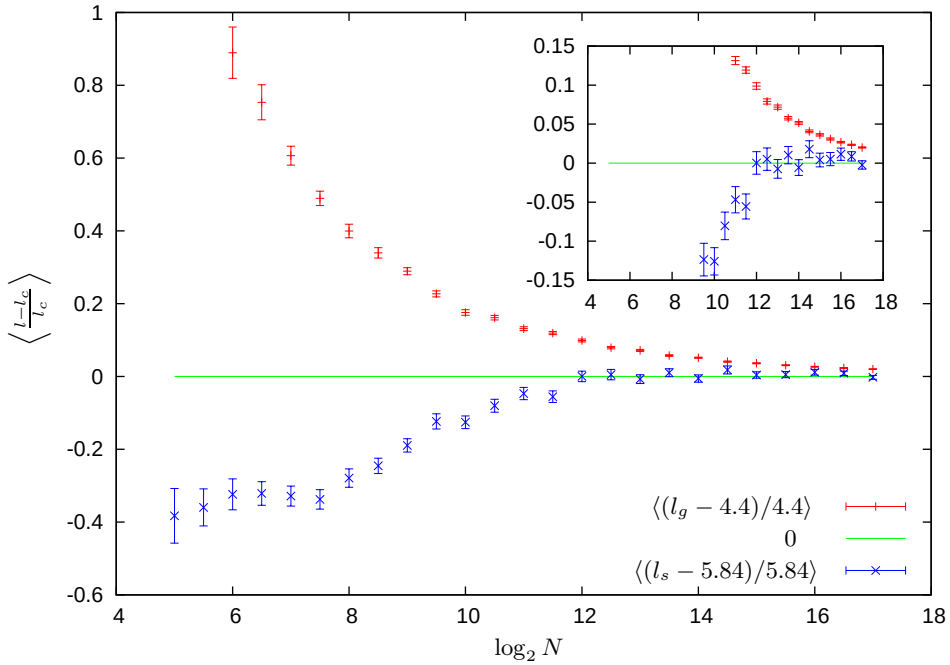

FIG. 10: Performance of diameter measures for an 'obtuse triangle', on causal sets sprinkled into an interval of $\mathbb{M}^3$. On the vertical axis, l stands for l_g or l_s, while l_c stands for 4.4 or 5.84, respectively. The inset plot zooms in on the asymptotic behavior.

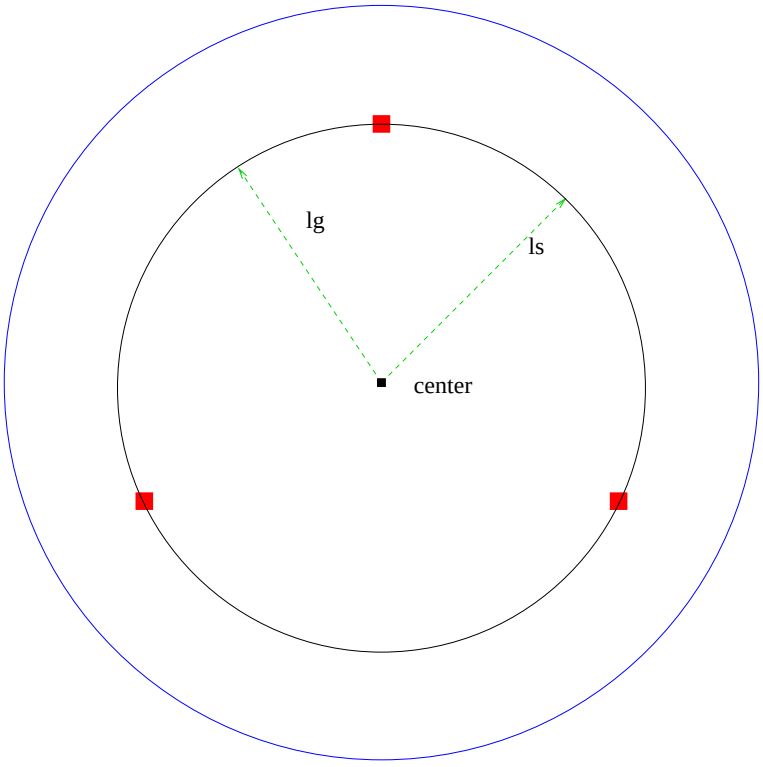

FIG. 11: Our acute triangle, in the $t = 0$ plane. The causal set is sprinkled into the causal interval with endpoints ($t = \pm 6.5614, x = y = 0$). The large blue circle is the intersection of the two lightcones which form the interval, and hence has radius 6.5614.

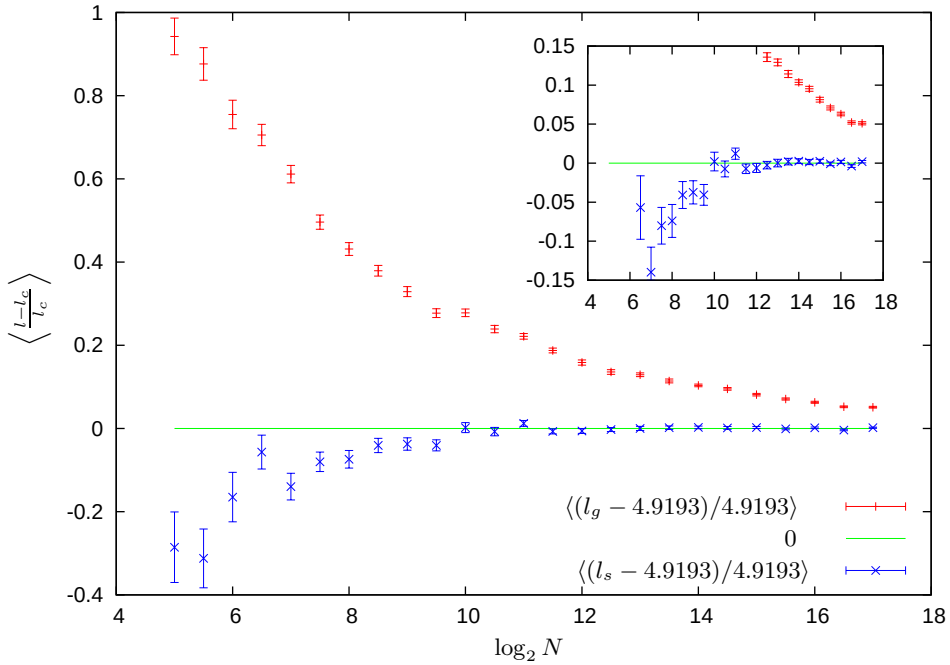

FIG. 12: Performance of diameter measures for an 'acute triangle', on causal sets sprinkled into an interval of $\mathbb{M}^3$. On the vertical axis, l stands for l_g or l_s, while l_c stands for 4.9193, respectively. The inset plot zooms in on the asymptotic behavior.

D. Remarks

Let us summarize and stress here a few issues before we move to a (quite) different proposal.

(a) The continuum distances l_g and l_s coincide if all the 'included angles' at the spacelike elements are 'acute' (or generally when the circumscribing and bounding sphere coincide).

(b) The accuracy of l_s does **not** depend on the included angles at the elements, and continues to give accurate results for obtuse angles.

(c) Even when l_s and l_g agree in principle (for acute angles) l_s gives a (slightly) more accurate value.

(d) By comparing l_s and l_g we can deduce whether, for example, the triangle (in 2+1-dimensions) formed by the elements is an obtuse or acute triangle. We therefore have, for acute triangles $l_s = l_g$, while for obtuse, $l_s > l_g$. Furthermore, one can deduce at which vertex the obtuse angle occurs, by examining the timelike distances $d(w, x_i)$ and $d(z, x_i)$ involved in the l_g computation. The element x_i which is furthest from w and z will be the one with the obtuse angle.

(e) l_g fails for obtuse triangles, in a similar manner as naive spatial distance, but much less severely. In particular, it does not converge to zero and in practice we expect the error to be usually quite small.

(f) l_s cannot be generalized easily in curved spacetimes, because it relies on (4.2), which was derived in flat spacetime. It cannot even be used for detecting nearest neighbors in a curved spacetime, despite the fact that for closest neighbors we can expect that things would be approximately flat. This is because we use equidistant elements, which may be far away, even for "nearby" unrelated elements.

We also mention three possible uses of the distances l_g, l_s in order to recover more geometric structure from the causal set.

(i) We can attempt to define *proximity* relations. For example, we can define balls around each element, and from this we may recover some of the underlying topology.

(ii) Given a particular inextendible antichain A (the discrete analogue of a spacelike hypersurface), one could perform the following procedure in order to find the element closest to any other given element. Select an

arbitrary element $x \in A$. Find the element $y \in A$ such that there does not exist any element $z \in A$ that makes xyz an obtuse triangle. This element y is then the closest neighbor to x within A [31].

One could repeat this procedure d times (for an antichain derived from a causet faithfully embeddable into $\mathbb{M}^d$) for each element $x \in A$, to form a d-valent adjacency graph for A. This graph then could be used for various purposes, *e.g.* to define spatial distance as the length of the shortest path connecting a pair of elements x and y.

(iii) Given a pair of unrelated elements x, y, one may attempt to define a spacelike distance in $\mathbb{M}^3$, by considering any element z that makes xzy an obtuse triangle with the obtuse angle at z. In that case l_g simply gives the 'longer leg' of the triangle, which is the distance between x and y. However this suggestion may fail because it depends on the third element. Minimizing over all possible third elements may bring back a similar problem as occurs with naive spatial distance. Even if one selects a third element randomly (such that an obtuse angle occurs at z), or averages over all possible such elements z, there is still the underestimation as mentioned above.[22]

V. SPATIAL DISTANCE

After having explored the difficulties with previous approaches, and obtained certain geometric information with some new constructions, we proceed by considering a quite different proposal, which is the main result of the paper.

A. Motivation and Definition

We come back to the initial problem of defining spatial distance. As explained in section II, it stems from the existence of many (in fact infinite) "minimizing pairs". In the previous section, we explored the possibility of obtaining some geometrical information by considering multiple (d) elements, whose common lightcones would intersect at a unique point. Here we take a different stance initiated by the following important observation. *Each minimizing pair (which lies close to a continuum minimizing pair) gives on average the correct expected distance.* All the problems arise when we minimize over these pairs. To use this observation to define a distance, we will need the following:

(a) a mechanism to select causet elements which lie close to a continuum minimizing pair. Such a mechanism involves

  (i) finding elements which are close to the intersection of the future (or past) light cones of our unrelated pair of elements

  (ii) for each such element z in the future (say), select an element w in the common past which locates a pair (w, z) which is close to some continuum minimizing pair.

(b) to take an **average** over minimizing pairs, and not minimize

As already described in section IV, 2-links will locate causet elements close to the intersection of the pair of light cones. Naively one may ask that, given a future 2-link f, select the past 2-link p that minimizes the timelike distance $d(p, f)$. However, this is unlikely to give a correct answer. Recall that in the continuum, for a given point on the common future lightcone, there exists a unique point on the common past lightcone that minimizes this distance. Future and past 2-links lie approximately on the intersection of the lightcones, but they are rare. Given a future 2-link f, it seems clear that in general there will be no past 2-link near the point on the past common lightcone that would minimize the distance $d(p, f)$. Therefore we propose the following procedure:

Step 1: Given spacelike elements x, y we find a future 2-link f_i.

Step 2: Find the element p_i in the common past of x and y that makes the timelike distance $d(p_i, f_i)$ minimum. This will select a minimizing pair.

---

[22] Note that these schemes would require identifying all of the infinite number of elements that form an obtuse angle. In addition, in higher dimensions, one would have to compose the appropriate generalization of this construction. These reasons make it not as appealing as the approach detailed in section V.

Step 3: Store the timelike distance $d^i(x, y)$ for the future 2-link f_i. Note that this distance can be calculated either as the length of the longest chain, or by using volume distance.

Step 4: Repeat for all other future 2-links.

Step 5: Take the average over all future 2-links $\langle d^i(x, y)\rangle$ to be the spacelike distance between elements x and y. We call this average the *2-link distance* between x and y.

To give some feel for the importance of using 2-links here, consider what would happen if in Step 1 we find a minimal element z to the common future of x and y, instead of a future 2-link. This element would be close to one of the future light cones of x or y, but not the other. Step 2 will yield a symmetrically placed element w in the common past. It is not difficult to see that the proper time separation between this pair w, z can be made arbitrarily large, by selecting an element z as far as one likes from the intersection of x and y's future light cones. Thus the 2-link construction plays a crucial role here in recovering the correct spatial distance.

For infinite Minkowski space, we expect to find an infinite number of 2-links, and thus this corresponds to taking an average over an infinite collection of (almost) independent random variables, each of which comes from the same underlying distribution. This gives a better and better approximation as we consider more pairs, and should give a well defined value in general (by the *central limit theorem* and the *law of large numbers*). To be complete, we must specify the order in which we add the terms in the average, in order for the infinite sum to be well defined. In our simulations (section V B), we consider future 2-links in order of their embedded time coordinate. Since the sprinkling domain is finite, it of course makes no difference. It seems clear that any 'reasonable' ordering of 2-links in this sum will work. We conjecture in particular that the order we use in the simulations will give a mean which converges to the spatial distance in the embedding, for a faithful embedding into infinite Minskowski space. More precisely, given a causal set which faithfully embeds into Minkowski space, with embedding ϕ, and any unrelated pair x and y, first select an arbitrary frame in which $\phi(x)$ and $\phi(y)$ are simultaneous, and then add the terms $d^i(x, y)$ above in order of increasing t-coordinate of $\phi(f_i)$. Alternatively, one can define an ordering of the terms that is independent of any embedding. For a finite region on Minkowski space, these subtleties do not arise.

Note that we could have used past 2-links instead and minimized over the common future. For a more symmetrical definition, we could average over both. With this procedure we evade the problem mentioned above, that in general there will be no past 2-link exactly on the point of the common past lightcones that would minimize the distance. Instead of looking to past 2-links, we simply select an element close to the relevant continuum point, by minimizing the geodesic distance. We are guaranteed to get a non-trivial result because, given a future 2-link, there exists a unique point in the continuum, to the common past, that minimizes the timelike geodesic distance. We avoid getting a degenerate distance in a similar way that we do not have problems in $1 + 1$ dimensions where there is a unique continuum pair. Finally, taking average over all the 2-links makes the distance less subject to fluctuations.

An important note is that for this procedure to work we need the 2-links to exist. As we have pointed out earlier (section IV), this is indeed the case for all dimensions greater than $1 + 1$. We could attempt to modify the definition in order to incorporate the $1 + 1$ case as well, but this may not be important, since in $1 + 1$ the naive spatial distance works anyway[23].

Before proceeding to see how this works with some simulations, we should point out that this distance function will overestimate the actual distance. This is the same effect that we called spacelike overestimation. This overestimation should always be comparable to the 'discreteness scale' (the spacing between embedded points), and thus should be negligible at large distances. In addition, the distance between two given elements should not be affected by considering portions of the causal set (faithfully embeddable into Minskowski space) which are far from the elements (in some given frame), unlike with naive spatial distance. Therefore, 'without loss of generality', we can consider a finite section of the full causal set, and get answers that should not be different from infinite causal sets.

B. Numerical results and comparison with naive spatial distance

The following plots compare 2-link distance with naive spatial distance.

The results shown in figure 13 are for simulations analogous to those whose results are shown in figure 7. We send the sprinkling density to infinity, while measuring the distance between two elements which are sprinkled near fixed target points at $t = 0, x = \pm 3/10, y = 0$, as described in section III B 1. Using coordinates for which the sprinkling

[23] The modification would be to consider "closest 2-neighbors", (defined suitably), rather than 2-links. For the case that there exist 2-links, the definition of "closest 2-neighbors" would coincide with 2-links.

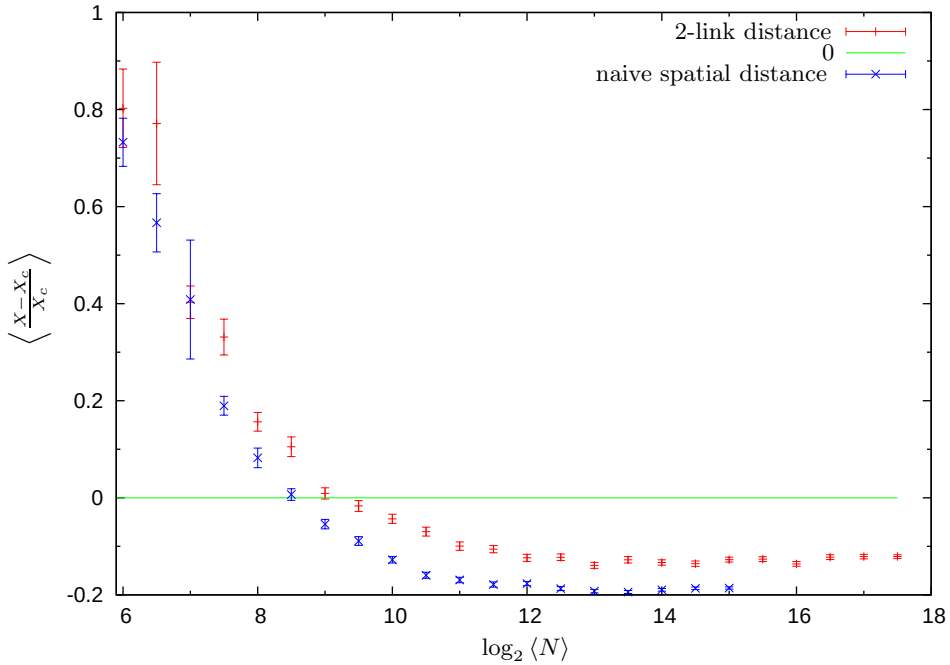

FIG. 13: Comparison of 2-link distance with naive spatial distance, for sprinklings into a fixed cube $[-1,1]^3$ in $\mathbb{M}^3$, for various densities $\rho \to \infty$. Target points are fixed at $(t=0, x=\pm\frac{3}{10}, y=0)$.

density ρ is fixed at 1, this means that we increase the distance between the target points, and observe that the 2-link distance converges to some constant small error, as the distance goes to infinity. For comparison we show the results of naive spatial distance on the same plot. We see that it behaves similarly. The effect of spacelike overestimation decreases rapidly for larger causal sets (larger distances in fundamental units). The naive spatial distance is always slightly less than the 2-link distance, since by definition it is obtained by taking the minimum over pairs of elements in the common past and future, so it cannot be less than a distance measure which employs an average over some subset of these pairs. The underestimation of naive spatial distance, that leads to its failure, is due to the existence of many (infinite) "minimizing pairs". However, given the way we select the sprinkling region, we take into account only relatively few independent minimizing pairs, and increasing N does not add more pairs because, in fundamental units, the distance also increases. Therefore, we do not expect to see an increasing discrepancy in the results. Note that both distances underestimate. This is likely due to timelike underestimation. Here we have used an asymptotic value for $m_3 = 2.27845$.

In figure 14, we compare the performance of 2-link distance with naive spatial distance, for the same sorts of causal sets used to generate figure 8. The two elements (or target points) are separated by a constant distance (in fundamental units), while we increase the volume of the region of Minkowski space into which we sprinkle. This results in considering more and more (independent) minimizing pairs. Here again we see that 2-link distance is not at all affected by the increasing size of the sprinkling region, as expected. The naive spatial distance, however, decreases as the sprinkling region grows, as noted earlier. This is the effect of taking into account more and more independent minimizing pairs, and selecting always the pair that gives the smallest distance. A good distance function should not be affected by the size of the region of Minkowski space into which we sprinkle (at least beyond some reasonable lower bound), when the two spacelike target points remain unchanged.

A final note on figure 14 is that the 2-link distance seems to overestimate the continuum distance. This is expected, since in fundamental units all the points of this plot correspond to a very small distance ($\lesssim 8$) (we can also compare with figure 13 the first points in the plot). For computational capacity reasons we could not do the same (increasing size of the sprinkling region, while holding the target points fixed) for a much larger distance (in fundamental units).

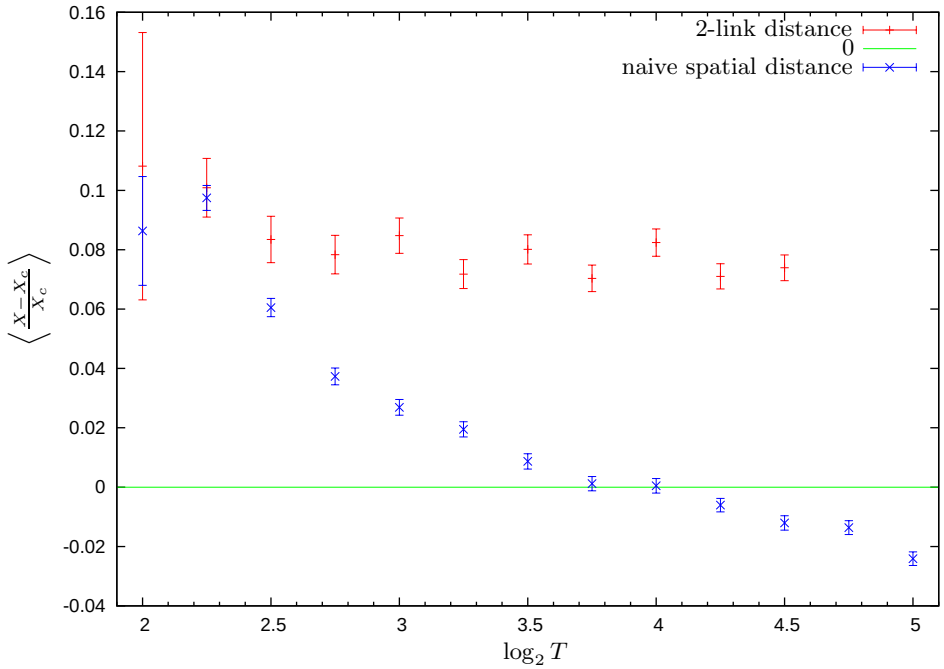

FIG. 14: Comparison of 2-link distance with naive spatial distance, for causets sprinkled into an expanding region $t \in (-T, T), x \in (-4, 4), y \in (-T, T)$ in $\mathbb{M}^3$, with target points at $(t = 0, x = \pm 4, y = 0)$. In these coordinates ρ is fixed at 1.

VI. TOWARD CURVED SPACETIME

A. Nearest neighbors

Having obtained a spacelike distance for causal sets which faithfully embed into Minkowski space, we turn to the question of whether we can define closest spatial neighbors. In the timelike direction, the closest neighbors are links. In a (somewhat) analogous manner we regard the spacelike neighbors of an element x as those whose 2-link distance from x is less than a small threshold. More formally, we wish to define a second, symmetric 's-link' relation on the elements of the causal set.

Definition 9: An *s-link* is the relation between a pair of elements of a causal set whose 2-link distance is less than a fixed threshold λ.

Any choice of λ (and whether to use volume distance or the length of the longest chain to measure timelike distance), will define the 's-link relation' on a causal set. By definition, the minimum possible value for 2-link distance is 2. Even for neighboring elements in the embedding, it is extremely unlikely that their 2-link distance will be exactly 2, as the fraction of 2-links which contribute anything to the sum in the mean besides 2 would have to be vanishingly small in the limit of infinite Minkowski space. We seek more 'typical' neighbors, and thus choose a threshold by the following procedure.[24]

1. Sprinkle N elements into a cube $[-1, 1]^3$ in $\mathbb{M}^3$ with $\langle N \rangle = 5793$.
2. Use the origin as a target point to select an element x.
3. Use the embedded location of this element as the target point to select a second element y. Here we take the closest y which is unrelated to x.
4. Repeat for 400 sprinklings, and compute the mean 2-link distance μ and its error $\delta\mu$.
5. Set $\lambda = \mu + \delta\mu = 2.186178$.

[24] Note that this procedure is not necessary, any reasonable value of λ (say below 3) can be used in practice.

Since we already have a notion of closest neighbor for related elements (namely links), we now have a definition for closest neighbors in general. Figure 15 shows how the s-links are distributed for a sprinkling into a cube of $\mathbb{M}^3$ with $< N >= 65536$. The element closest to the center of the cube is our reference, and the blue elements are all the s-links from that element. As expected, they tend to lie on a hyperboloid.

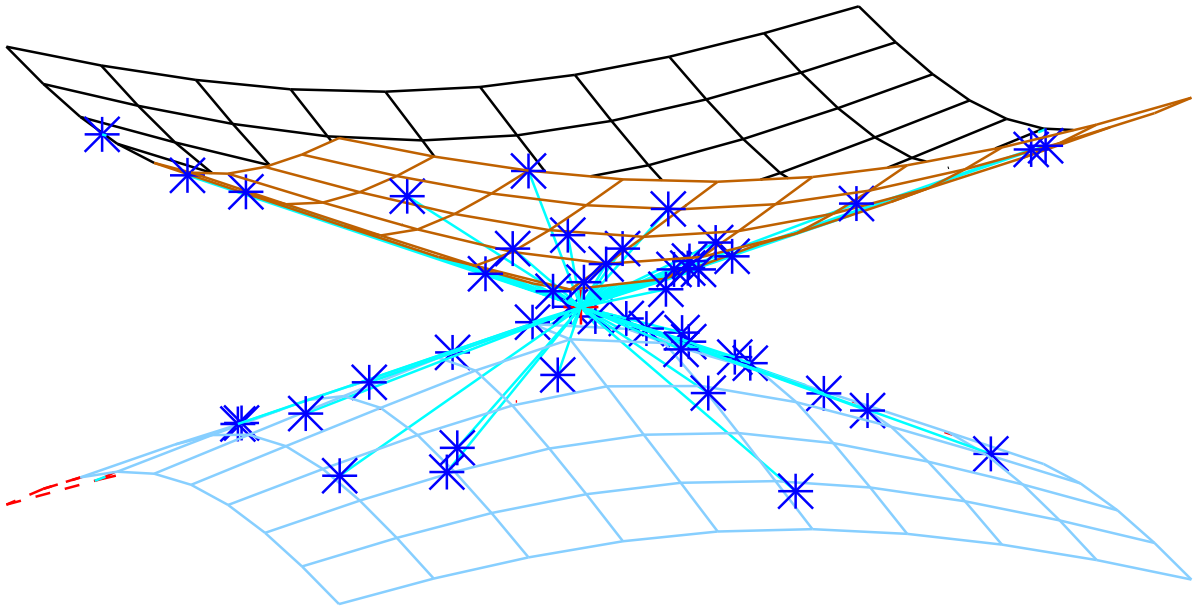

FIG. 15: Spatial nearest neighbors of an element in a sprinkling into (a fixed cube in) $\mathbb{M}^3$. $\langle N \rangle = 65\,536$. The future and past light cones of the 'origin element' x are shown. The spacelike cyan lines are drawn between x and each neighbor, for emphasis.

B. Spatial distance in curved spacetime

In the continuum, one defines a curve as a smooth map from a connected subset of the real line to the manifold $\mathcal{M}$. The analogue of a curve, in a causal set, would be a sequence of elements, *i.e.* a map from (a subset of) $\mathbf{N}$ to the causal set $\mathcal{P}$.

It is obvious that the smoothness condition cannot be implemented. However, we *can* have a continuity condition. Intuitively, we require that the curve be composed of a sequence of elements for which each successive pair are 'nearest neighbors', in either the timelike (link) or spacelike (s-link) sense. To properly define continuity, one needs to specify the topology on the causal set $\mathcal{P}$, and on the natural numbers $\mathbf{N}$. However, an obvious problem is that both domain and range are "locally finite", which implies that natural choices (*e.g.* order topology or open ball topology respectively) will lead to the discrete topology in which case *any* map is continuous. The correct construction of the appropriate topology, which despite being discrete captures continuum notions, is described in [32], and similar arguments were also used in [13]. The result of that construction applied to our case is that a curve is "continuous" if it maps any two consecutive numbers of the $\mathbf{N}$ to elements in $\mathcal{P}$ that are related as "closest-neighbors", *i.e.* are either links or s-links. Further details on this are beyond the scope of this paper and the reader is referred to the original references.

Having defined what we mean by continuous curve, we can easily define the length of a curve, as simply its cardinality. An important thing to note here is that we have now defined the length of continuous curves in a causal set, which need *not* be solely timelike or solely spacelike, but can also be mixed, *i.e.* at some points spacelike and other points timelike.[25]

So far we have only considered causal sets that are well approximated by Minkowski spacetime. One of the virtues of this discussion is that it could be generalized for curved spacetimes. In particular, assuming that the spacetime

[25] In [13] the spatial topology of a causal set was recovered (with drastically different methods than ours). The possibility of defining continuous spacelike curves, something that was not possible earlier, could be recovered. However the case of general continuous curves is something that could not be obtained.

is approximately flat at some small scale above the Planck scale but much below the macroscopic scales (*i.e.* locally flat), we can use the above construction to define closest neighbors (s-links). The idea would be to consider some region, for example an order interval, whose size is comparable to this local flatness scale. One would then sum over only the 2-links which lie within this local region. Since the determination of an s-link in this manner depends only on a local subset of the causal set (in any frame for which local flatness is valid), it seems likely that any construction that is based on the closest neighbors, such as length of a continuous curve, will carry over to (causets which faithfully embed into) curved spacetime. A very similar strategy has been employed to write down an action functional for a causal set with a scalar field [26]. See also [33], for a similar approach to extracting geometry from the causal structure of a locally flat region. Note that in curved spacetime the concept of spacelike distance between two points is not well defined in general, but the length of a (smooth) curve is.

If we restrict attention to an inextendible antichain, analogous to a spatial hypersurface, the definition of closest neighbors can give a spatial distance, defined as the graph distance between two elements, where the graph edges coincide with the s-links between elements of the antichain. This distance is what one would expect from minimizing the length of the possible (continuous) spacelike curves. Note that there is a direct analogy with the continuum case (where spatial distance between two points is indeed the length of the minimum curve between those points).

Figure 16 depicts such a graph, for a 'smooth' inextendible antichain at the 'center' of a $\langle N \rangle = 1024$ element causal set faithfully embedded into a cube in $\mathbb{M}^3$.[26] Since the inextendible antichain has much fewer elements than the causal set, it is necessary to use a larger threshold to define adjacency, as otherwise very few pairs will be regarded as adjacent in the antichain. Here we use 2.7. The picture of the graph was generated by the Graphviz package [36].

Finally, one can speculate wildly, about how one may be able to recover tangent spaces and thus the full metric on a causal set. This is left for future work, but here we just point out some observations and a potential problem.

One could consider that for a given element x, each of the closest neighbors are possible "vectors", since we can consider them as equivalence classes of continuous curves (each with the same tangent at x). Moreover, if we consider the limit of infinite sprinkling density, we expect that these vectors will form a dense set. Therefore in some sense we cover all the directions, at least in the large density limit. However, for all this to make sense, we need to define the tangent space as a vector space (in order to define vector fields, and thus a metric tensor). To do this one must somehow define a closed operation of vector addition, without resorting to the background structure. Perhaps one could make progress by considering the angles between vectors (which could be done using our definitions of timelike and spacelike distances).

VII. SUMMARY AND CONCLUSIONS

We have discussed various ways of recovering geometrical information of continuum spacetime from a causal set that the spacetime approximates. All of the constructions involved causal sets that are approximated by Minkowski spacetime, however some remarks about generalization to curved spacetime appear in section VI B.

In particular we began by reviewing and numerically testing some previous definitions (*e.g.* from [10]), namely on timelike and spacelike distance. The timelike distance between two elements is proportional to the length of the longest chain connecting them (for large N). From our simulations we extracted the asymptotic value of the proportionality constant m_3 (m_2 is known to be 2) and computed the value of m_d^{eff} (for $d = 2, 3$), which is an effective proportionality constant relevant for finite timelike distances. Furthermore we examined the naive spatial distance, which is defined to be the smallest timelike distance between the common past and common future of the two unrelated elements in question. As argued in [10], this fails to recover the continuum spacelike distance, due to the existence of infinite "independent minimizing pairs". We observed evidence of this failure numerically for finite causal sets.

The second part of our paper concerned some new ideas. First we defined the concept of an n-link. This is defined to be any element that is linked to n-unrelated elements. It essentially captures the notion of points lying on the light-cones of *all* n-unrelated (*i.e.* spacelike) elements. It was shown that in d dimensions, for n unrelated elements, where $n \leq d-1$, we find an infinite number of n-links, while for $n \geq d$ we generally find none (for a given n elements). This can help us determine the dimension of the causal set, since the smallest n for which we find no n-links is equal to the dimension ($n = d$). It may also serve as an indicator of 'manifoldlike' causal sets, as the numbers of n-links should behave in this particular manner for faithfully embeddable causets.

---

[26] The inextendible antichain was generated using the thickening technique described in [35]. Starting from the minimal elements, we thicken to $v = 98$, and take the maximal elements A of this thickened antichain. Since in general this will not form an inextendible antichain, we must extend it by adjoining the minimal elements of the complement of $A \cup \text{fut}(A) \cup \text{past}(A)$.

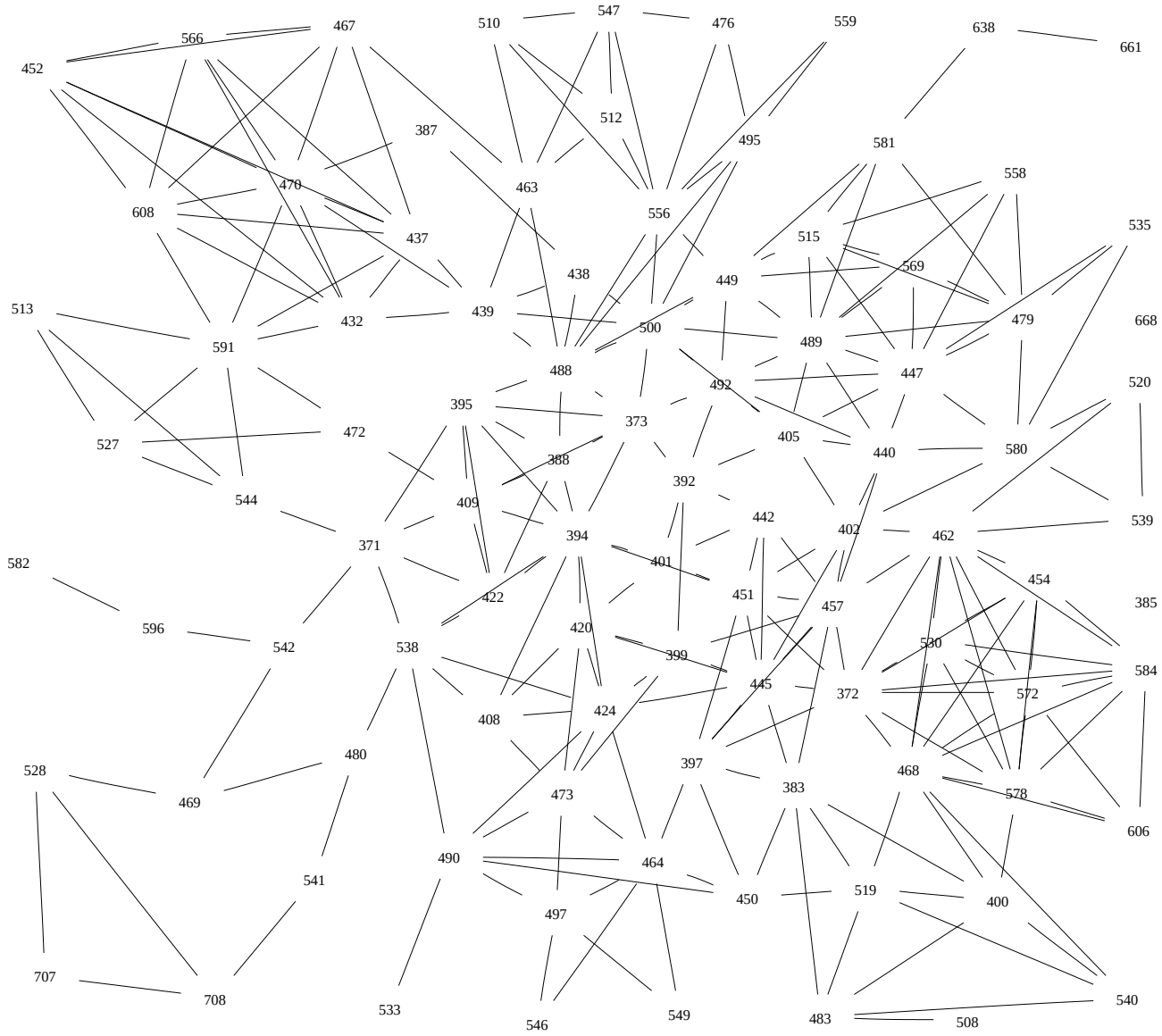

FIG. 16: Graph formed from nearest neighbors in a 'smooth' inextendible antichain, at the center of a causal set faithfully embedded into a box in $\mathbb{M}^3$, of spacetime volume 1024. The nearest neighbor threshold is set to 2.7.

For d unrelated elements in $\mathbb{M}^d$ we defined the "generalized spatial distance" l_g, which corresponds to the diameter of the bounding sphere of those elements. Using the concept of *equidistant* elements, we defined the "sphere distance" l_s, which computes the diameter of the *circumscribing* sphere of the d-unrelated elements. In 2+1 dimensions, noting that the circumscribing and the bounding spheres coincide when all the angles at the elements are acute, we can deduce whether there is an obtuse angle by comparing l_g with l_s. In arbitrary dimension d, the statement that all angles are acute can be expressed more generally as the statement that the center of the $d-2$-sphere defined by the d elements lies within their convex hull.

The third part of this paper (and the main result), was to define "'spatial distance", and furthermore to define spatial closest neighbors, called *s-links*. This was done by making the observation that each minimizing pair gave the correct distance, and the problem arose when we minimized over all those pairs. In this proposal, we had to (a) select relevant pairs, and (b) take an average over their (timelike) distance. To select the relevant pairs we used crucially the concept of a 2-link, that lies close to the intersection of the lightcones. We then numerically tested this suggestion in $\mathbb{M}^3$, and found it to give good distances (close to the continuum ones), and most importantly it did *not* suffer from the same problem of underestimation of the naive spatial distance (*cf.* figure 14). We then used this definition to

define "s-links", being the analogues of links for unrelated elements. In finding the s-links, we are working locally, and thus we may expect that these considerations can be generalized directly to curved spacetimes. In both cases (flat/curved) knowing the closest neighbors (timelike and spacelike) allows us to define the length of a (continuous) curve. This is an important step to the recovery of the full curved spacetime geometry.

Given such a full recovery of spacetime geometry from a causal set (which is yet to be achieved), one could likely do the following.

(a) Prove the "Hauptvermutung", which is the main conjecture of the causal set program. It claims that two distinct, non-isometric spacetimes cannot arise from a single causal set.

(b) Given a causal set, we will be in position to tell if it corresponds to a spacetime, and which is the corresponding metric. This will guide us as to whether the quantum dynamics we impose leads to physical predictions that agree with observation!

(c) It would be possible to write down the Einstein action in terms of causal set quantities. This may be used to "naively quantize" by computing sums over causal sets with the appropriate amplitudes.

On a more immediate time frame, these extra structures that we can compute from a causal set could be useful in a number of ways. One could, for example, use these (*e.g.* the n-links, spatial distance, or the length of curves) to more readily derive entropy bounds and compute black hole entropy from causal sets (as in [34]), because they allow one to more readily identify the relevant substructures of the causal set to count.

VIII. ACKNOWLEDGMENTS

We are especially grateful to Graham Brightwell for a number of discussions on this work, for example in leading us toward the relevant parameters required to demonstrate the failure of naive spatial distance on the computer. We are also grateful to Rafael Sorkin, David Meyer, and the attenders of 'relativity lunch' at Imperial College London, for numerous helpful discussions. We thank the anonymous referees for numerous constructive remarks and suggestions.

We thank Yaakoub El-Khamra for his patient assistance with our parallel Monte Carlo code.

This research was supported by a number of grants/organizations, including the Marie Curie Research and Training Network ENRAGE (MRTN-CT-2004-005616), the Royal Society International Joint Project 2006-R2, and the Perimeter Institute for Theoretical Physics. Research at Perimeter Institute is supported by the Government of Canada through Industry Canada and by the Province of Ontario through the Ministry of Research & Innovation.

Many of the numerical results were made possible by the facilities of the Shared Hierarchical Academic Research Computing Network (SHARCNET:www.sharcnet.ca).

PW thanks the Perimeter Institute for Theoretical Physics for hospitality.

APPENDIX A: PROOF OF EXISTENCE OF EQUIDISTANT ELEMENTS IN 1+1 DIMENSIONS

Here we prove the existence of equidistant elements in 1+1 dimensions. In higher dimensions the proof gets much more complicated. We rely on numerical evidence and the intuition obtained from the 1+1 dimensional case to suggest that they also exist generically in higher dimensions.

We are looking for equidistant elements in 1+1 dimensions between causet elements mapped to points $x_1 = (-r, -r)$ and $x_2 = (-r, r)$, for some faithful embedding. First we note is that in 1+1 dimensions the order intervals between a point y in the common future ($J_c^+ := J^+(x_1) \cap J^+(x_2)$) and x_1 and x_2 are divided into one common region and two disjoint regions. For an element to be equidistant, since there are obviously an equal number of elements in the common region, it suffices to show that the independent regions have same number of elements mapped to them. These independent regions are defined by the coordinates of the point y in the common future.

Let us move to lightcone coordinates for which $x_1 = (-\alpha, o)$, $x_2 = (0, -\alpha)$ and $\alpha = r\sqrt{2}$. Given a point in the common future with coordinates $y = (u, v)$, it is clear that the area of the region $[x_1, y]_c \setminus [x_2, y]_c$ (*i.e.* the area causally between x_1 and y after we subtract the overlap with the region $[x_2, y]_c$) is equal to $V_1 = \alpha u$ and similarly $[x_2, y]_c \setminus [x_1, y]_c$ has area $V_2 = \alpha v$. Note again that the contents of $[x_1, y]_c$ and $[x_2, y]_c$ are independent for any u and v. We can now compute the following:

(a) The expected number of elements $E(n \in [x_1, y]_c)$ in the common future J_c^+, such that the region $[x_1, y]$ contains exactly n elements[27] :

$$\langle E(n \in [x_1, y]_c) \rangle = \int_0^\infty du dv \frac{(\alpha v)^n}{n!} \exp(-\alpha v) = \int_0^\infty du \frac{1}{\alpha} \to \infty$$

(b) The expected number of elements in the common future J_c^+, such that the region $[x_1, y]$ contains exactly n elements **and** the region $[x_2, y]$ also has exactly n elements:

$$\begin{aligned} \langle E(n \in [x_1, y]_c \text{ and } n \in [x_2, y]_c) \rangle &= \int_0^\infty dv dv \left(\frac{(\alpha v)^n}{n!} \exp(-\alpha v) \right) \left(\frac{(\alpha u)^n}{n!} \exp(-\alpha u) \right) \\ &= \frac{1}{\alpha^2} \end{aligned} \tag{A1}$$

The expected number of equidistant elements $E(\text{equidistant})$ is then recovered when we add (A1) for all possible values of n, in other words

$$\langle E(\text{equidistant}) \rangle = \sum_{n=0}^{\infty} \frac{1}{\alpha^2} \to \infty \, . \tag{A2}$$

This completes the proof of the existence of infinite equidistant elements in 1+1 dimensions.

Note 1: In higher dimensions the proof is more difficult since the simplifying features of using the lightcone coordinates do not apply.

Note 2: $\frac{1}{\alpha^2} \propto \frac{1}{r}$, so if $r \to \infty$ (A2) is not well defined. For any finite distance between the two points, the above argument holds.

Note 3: Both points (a) and (b) above are to be expected. Intuitively there will be some v such that $[x_1, y]_c$ contains exactly n elements. On average we expect that $v\alpha = n$. One can then find another y' whose v coordinate is $v + \delta v$, such that $[x_1, y']_c$ contains exactly $n+1$ elements, and on average $(v + \delta v)\alpha = n + 1$. Thus we expect on average $\delta v = 1/\alpha$. However any element in the whole region between v and $v + \delta v$ for **any** u will give us elements which find exactly n elements in $[x_1, y]_c$. Since the above area is infinite, the expected number is infinite.

An analogous argument gives an expected value for $\delta u = 1/\alpha$. If we require that both $[x_1, y]_c$ and $[x_2, y]_c$ have exactly n elements, we end up considering the area $\delta u \cdot \delta v = \frac{1}{\alpha^2}$. Thus the expected elements in J_c^+ that have exactly n elements in both $[x_1, y]_c$ and $[x_2, y]_c$ comes naturally to be $1/\alpha^2$.

---

[1] Jan Myrheim, "Statistical Geometry", CERN preprint Ref.TH.2538-CERN (1978).

[2] G. 't Hooft, "Quantum gravity: A fundamental problem and some radical ideas," in *Recent Developments in Gravitation (Proceedings of the 1978 Cargese Summer Institute)*, M. Levy and S. Deser, eds. Plenum, 1979.

[3] L. Bombelli, J.H. Lee, D. Meyer, and R. Sorkin, "Space-time as a causal set," *Phys. Rev. Lett.* **59** (1987) 521.

[4] J. Ambjørn and R. Loll, "Non-perturbative Lorentzian quantum gravity, causality and topology change", *Nucl. Phys. B* **536** (1998) 407. [hep-th/9805108].

[5] T. Thiemann, *Introduction to Modern Canonical Quantum General Relativity*, Cambridge University Press, Cambridge 2006. ⟨e-print arXiv: gr-qc/0110034⟩.

[6] J. Baez, "Spin Foam Models", *Class. Quant. Grav.***15**, 1827–1858 (1998). ⟨e-print arXiv: gr-qc/9709052⟩.

[7] T. Konopka, F. Markopoulou and L. Smolin, "Quantum graphity," arXiv:hep-th/0611197.

[8] W. M. Stuckey and M. Silberstein, "Unification per the Relational Blockworld" (2007). ⟨e-print arXiv: 0712.2778 [quant-ph]⟩.

---

[27] using that $\int_0^\infty x^n \exp(-ax) dx = \frac{n!}{a^{n+1}}$.

[9] Lee Smolin, "The case for background independence", in Rickles, D. (ed.) et al.: *The structural foundation of quantum gravity* 196–239. (2005). ⟨e-print arXiv: hep-th/0507235⟩.

[10] G. Brightwell and R. Gregory, "The Structure of Random Discrete Spacetime", , Phys. Rev. Lett. 66: 260-263 (1991).

[11] E. Bachmat, "Discrete spacetime and its applications," arXiv:gr-qc/0702140.

[12] L. Bombelli, J. Henson and R. D. Sorkin, "Discreteness without symmetry breaking: A theorem," arXiv:gr-qc/0605006.

[13] S. Major, D. Rideout, and S. Surya, "On recovering continuum topology from a causal set," *J. Math. Phys.* **48, 032501** (2007). ⟨e-print arXiv: gr-qc/0009063⟩.
Sumati Surya, "Causal Set Topolgy" , *Theoretical Computer Science* **405**, 1–2, pp. 188–197 (2008). ⟨e-print arXiv: 0712.1648 [gr-qc]⟩.

[14] Joe Henson, "Constructing an interval of Minkowski space from a causal set", ⟨e-print arXiv: gr-qc/0601069⟩ (2006).

[15] R. Ilie, G. B. Thompson and D. D. Reid, "A numerical study of the correspondence between paths in a causal set and geodesics in the continuum," Class. Quant. Grav. **23**, 3275 (2006).

[16] G. Brightwell, J. Henson and S. Surya, "A 2D model of Causal Set Quantum Gravity: The emergence of the continuum," (2007). ⟨e-print arXiv: 0706.0375 [gr-qc]⟩.

[17] Steven Johnston, "Particle propagators on discrete spacetime" (2008). ⟨e-print arXiv: 0806.3083 [hep-th]⟩.

[18] R. D. Sorkin, "Is the cosmological 'constant' a nonlocal quantum residue of discreteness of the causal set type?," AIP Conf. Proc. **957**, 142 (2007) ⟨e-print arXiv: 0710.1675 [gr-qc]⟩.

[19] R. D. Sorkin, "Does locality fail at intermediate length-scales?", to appear in *Towards Quantum Gravity*, D. Oriti (ed.), Cambridge University Press. ⟨e-print arXiv: gr-qc/0703099⟩.

[20] R. D. Sorkin, "Space-time and causal sets," in *Relativity and Gravitation: Classical and Quantum (Proceedings of the SILARG VII Conference, Cocoyoc, Mexico, December 1990)*, pp. 150–173. World Scientific, Singapore, 1991.

[21] R. D. Sorkin, "First steps with causal sets," in *Proceedings of the ninth Italian Conference on General Relativity and Gravitational Physics, Capri, Italy, September 1990*, R. Cianci, R. de Ritis, M. Francaviglia, G. Marmo, C. Rubano, and P. Scudellaro, eds., pp. 68–90. World Scientific, Singapore, 1991.
F. Dowker, "Causal sets and discrete spacetime," AIP Conf. Proc. **861**, 79 (2006).

[22] R. D. Sorkin, "Causal sets: Discrete gravity," in *Lectures on Quantum Gravity, Proceedings of the Valdivia Summer School, Valdivia, Chile, January 2002*, A. Gomberoff and D. Marolf, eds. Plenum, 2005. ⟨e-print arXiv: gr-qc/0309009⟩.

[23] J. Henson, "The causal set approach to quantum gravity," in *Approaches to Quantum Gravity – Towards a new understanding of space and time*, D. Oriti, ed. Cambridge University Press, 2006. ⟨e-print arXiv: gr-qc/0601121⟩.

[24] R. D. Sorkin, "Is the cosmological 'constant' a nonlocal quantum residue of discreteness of the causal set type?," AIP Conf. Proc. **957**, 142 (2007) ⟨e-print arXiv: 0710.1675 [gr-qc]⟩.
M. Ahmed, S. Dodelson, P. B. Greene and R. Sorkin, "Everpresent Lambda," Phys. Rev. D **69**, 103523 (2004) ⟨e-print arXiv: astro-ph/0209274⟩.

[25] J. Henson, "Quantum Histories and Quantum Gravity", in preparation (2008).

[26] Roman Sverdlov and Luca Bombelli, "Gravity and Matter in Causal Set Theory", (2008). ⟨e-print arXiv: 0801.0240 [gr-qc]⟩.

[27] D.A. Meyer, "Spherical containment and the Minkowski dimension of partial orders", *Order* **10** 227–237 (1993).
———, *The Dimension of Causal Sets*, PhD Thesis, M.I.T. (1988).
D. D. Reid, "The manifold dimension of a causal set: Tests in conformally flat space-times," Phys. Rev. D **67**, 024034 (2003).

[28] Jinho Baik, Percy Deift, and Kurt Johansson, "On the Distribution of the Length of the Longest Increasing Subsequence of Random Permutations," J. Amer. Math. Soc. **12**, No. 4, pp 1110–1178 (1999).

[29] T. Goodale, G. Allen, G. Lanfermann, J. Massó, T. Radke, E. Seidel, and J. Shalf, "The Cactus Framework and Toolkit: Design and Applications" in *Vector and Parallel Processing — VECPAR 2002, 5th International Conference*, Springer, pp. 197–227.

[30] Pierre L'Ecuyer, "Combined Multiple Recursive Random Number Generators", *Operations Research*, Vol. 44, No. 5. (Sep. – Oct., 1996), pp. 816–822.

[31] Graham Brightwell, private communication.

[32] Rafael D. Sorkin, "A Finitary Substitute For Continuous Topology", Int. J. Theor. Phys. **30**, 923 (1991).

[33] G. W. Gibbons and S. N. Solodukhin, Phys. Lett. B 649: 317-324 (2007).

[34] D. Dou and R. D. Sorkin, Found. Phys. **33**, 279 (2003); D. Rideout and S. Zohren, Class. Quant. Grav. **23**, 6195 (2006).

[35] S. Major, D. Rideout, and S. Surya, "Spatial hypersurfaces in causal set cosmology," Class. Quant. Grav. **23**, 4743 (2006). ⟨e-print arXiv: gr-qc/0506133⟩.

[36] `www.graphviz.org`